ELECTRIC PROPULSION

As mentioned in Chapters 1 and 2, electric rocket propulsion devices use electrical energy for heating and/or directly ejecting propellant, utilizing an energy source that is independent of the propellant itself. The purpose of this chapter is to provide an introduction to this field. Vector notation is used in several of the background equations presented.

The basic subsystems of a typical electric propulsion thruster are: (1) a raw energy source such as solar or nuclear energy with its auxiliaries such as concentrators, heat conductors, pumps, panels, radiators, and/or controls; (2) conversion devices to transform this energy into electrical form at the proper voltage, frequency, pulse rate, and current suitable for the electrical propulsion system; (3) a propellant system for storing, metering, and delivering the propellant; and (4) one or more thrusters to convert the electric energy into kinetic energy of the exhaust. The term thruster is commonly used here, as thrust chamber is in liquid propellant rockets.

Electric propulsion is unique in that it includes both thermal and non-thermal systems as classified in Chapter 1. Also, since the energy source is divorced from the propellant, the choice of propellant is guided by factors much different to those in chemical propulsion. In Chapter 3, ideal relations that apply to all thermal thrusters are developed which are also relevant to thermal-electric (or electrothermal) systems. Concepts and equations for non-thermal-electric systems are defined in this chapter. From among the many ideas and designs of electric propulsion devices reported to date, one can distinguish the following three fundamental types:

- 1. *Electrothermal*. Propellant is heated electrically and expanded thermodynamically; i.e., the gas is accelerated to supersonic speeds through a nozzle, as in the chemical rocket.
- 2. *Electrostatic*. Acceleration is achieved by the interaction of electrostatic fields on non-neutral or charged propellant particles such as atomic ions, droplets, or colloids.
- 3. *Electromagnetic*. Acceleration is achieved by the interaction of electric and magnetic fields within a plasma. Moderately dense plasmas are high-temperature or nonequilibrium gases, electrically neutral and reasonably good conductors of electricity.

A general description of these three types was given in Chapter 1, Figs. 1–8 to 1–10. Figure 19–1 and Tables 2–1 and 19–1 show power and performance values for several types of electric propulsion units. Note that the thrust levels are small relative to those of chemical and nuclear rockets, but that values of specific impulse can be substantially higher; the latter may translate into a longer operational life for satellites whose life is presently propellant limited. Inherently, electric thrusters give accelerations too low for overcoming the high-gravity field of earth launches. They function best in space, which also

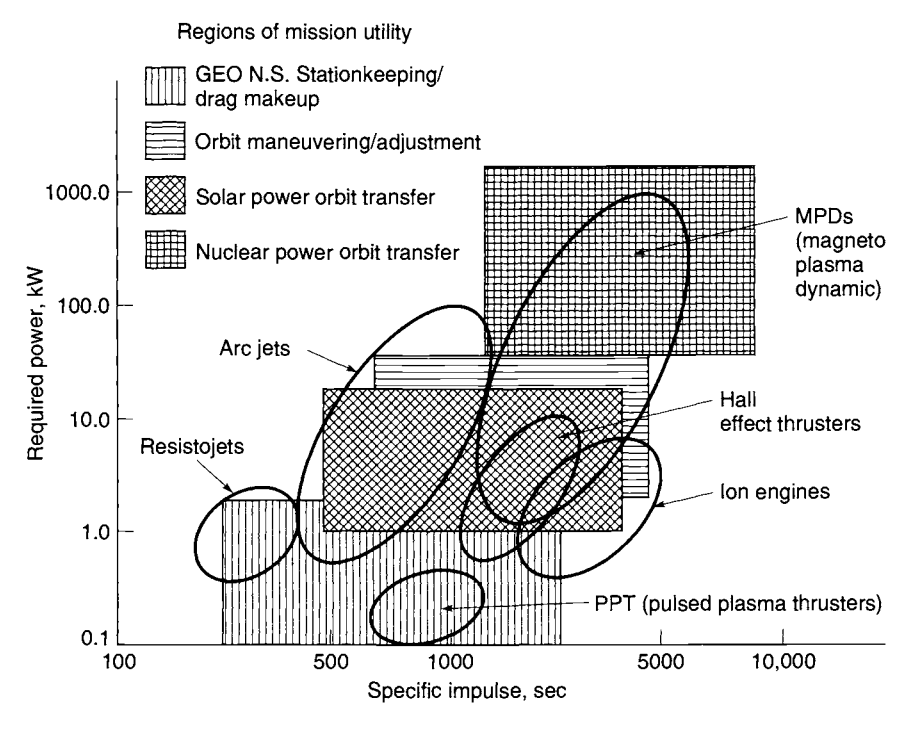


FIGURE 19–1. Overview of the approximate regions of application of different electrical propulsion systems in terms of power and specific impulse.

TABLE 19-1. Typical Performance Parameters of Various Types of Electrical Propulsion Systems

Туре	Thrust Range (mN)	Specific Impulse (sec)	Thruster Efficiency ^b (%)	Thrust Duration	Typical Propellants	Kinetic Power per Unit Thrust (W/mN)
Resistojet (thermal)	200–300	200-350	65–90	Months	NH ₃ ,N ₂ H ₄ ,H ₂	0.5-6
Arcjet (thermal)	200-1000	400-1000	30-50	Months	H_2, N_2, N_2H_4, NH_3	2-3
Ion engine	0.01 - 200	1500-5000	60-80	Months	Xe,Kr,Ar	10-70
Solid pulsed plasma (PPT)	0.05-10	600-2000	10	Years	Teflon	10-50
Magnetoplasma dynamic (MPD)	0.001 - 2000	2000-5000	30-50	Weeks	Ar,Xe,H ₂ ,Li	100
Hall thruster	0.01~2000	1500-2000	3050	Months	Xe,Ar	100
Monopropellant rocket"	30–100,000	200–250	87–97	Hours or minutes	N_2H_4	

^aListed for comparison only. ^bSee Eq. 19–3.

matches the near-vacuum exhaust pressures required of electrostatic and electromagnetic systems. All flight missions envisioned with electric propulsion operate in a reduced-gravity or gravity-free space and, therefore, must be launched from earth by chemical rocket systems.

The many advantages of electric propulsion had been offset by their required use of substantial quantities of electricity which, at certain power levels, had been an expensive commodity in space until recently. All types of electric propulsion presently depend on a vehicle-borne power source—based on solar, chemical, or nuclear energy—and power conversion and conditioning equipment. The mass of the electric generating equipment, even when solar energy is employed, can become much larger than that of the thrusters, particularly when thruster efficiency is low. This causes appreciable increases in inert-vehicle mass (or dry-mass). Modern satellites and other spacecraft have substantial communications requirements. Typically these satellites can share their electrical power sources, thus avoiding the penalty to the propulsion system. What remains to be tagged to the propulsion system is the power-conditioning equipment, except in instances where it is also shared with other spacecraft components.

Electric propulsion has been considered for space applications since the inception of the space program in the 1950s but has only begun to make widespread impact since the mid-1990s. This is a result of the availability of sufficiently large amounts of electrical power in spacecraft. References 19–1 to 19–3 are devoted to electric propulsion. Basic principles on electric propulsion devices are given in these references, along with applications, although the information relates to older versions of such devices. Table 19–2 gives a comparison of advantages and disadvantages of several types of electric propulsion. Pulsed devices differ from continuous or steady-state in that startup and shutdown transients may degrade their effective performance. Pulsed devices, however, are of practical importance, as is detailed later in this chapter.

The *applications* for electric propulsion fall into several broad mission categories (these have already been introduced in Chapter 4):

- (1) Overcoming translational and rotational perturbations in satellite orbits, such as north-south station keeping (NSSK) of satellites in geosynchronous orbits (GEO) or aligning telescopes or antennas or drag compensation of satellites in low (LEO) and medium earth orbits (MEO). For a typical north-south station-keeping task in a 350-km orbit, a velocity increment of about 50 m/sec every year or 500 m/sec for 10 years might be needed. Several different electric propulsion systems have actually flown in this type of mission.
- (2) Increasing satellite speed while overcoming the relatively weak gravitational field some distance away from the earth, such as *orbit raising* from a low earth orbit (LEO) to a higher orbit or even to a geosynchronous orbit (GEO). Circularizing an elliptical orbit may require 2000 m/sec and going from LEO to GEO typically might require a velocity increase

TABLE 19-2. Comparison of Electrical Propulsion Systems

Type	Advantages	Disadvantages	Comments
Resistojet (electrothermal)	Simple device; easy to control; simple power conditioning; low cost; relatively high thrust and efficiency; can use many propellants, including hydrazine augmentation	Lowest I _s ; heat loss; gas dissociation; indirect heating of gas; erosion	Operational
Arcjet (electrothermal & electromagnetic)	Direct heating of gas; low voltage; relatively simple device; relatively high thrust; can use catalytic hydrazine augmentation; inert propellant	Low efficiency; erosion at high power; low I_s ; high current; heavy wiring; heat loss; more complex power conditioning	High-thrust units need P_e of 100 kW or more. Operational
Ion propulsion (electrostatic)	High specific impulse; high efficiency; inert propellant (xenon)	Complex power conditioning; high voltages; single propellant only; low thrust per unit area; heavy power supply	Flown in satellites (DS1)
Pulsed plasma (PPT) (electromagnetic)	Simple device; low power; solid propellant; no gas or liquid feed system; no zero-g effects on propellant	Low thrust; Teflon reaction products are toxic, may be corrosive or condensable; inefficient	Operational
MPD Steady-state plasma (electromagnetic)	Can be relatively simple; high I_s ; high thrust per unit area	Difficult to simulate analytically; high specific power; heavy power supply	Several have flown
Hall thruster (electromagnetic)	Desirable I _s range; compact, relatively simple power conditioning; inert propellant (Xe)	Single propellant; high beam divergence; erosion	Operational

- of up to 6000 m/sec. Several electric propulsion units are being developed for these types of mission.
- (3) Potential missions such as *interplanetary travel* and *deep space probes* are also candidates for electric propulsion. A return to the moon, missions to Mars, Jupiter, and missions to comets and asteroids are of present interest. These all require relatively high thrust and power. A few electric thrusters for this category of missions (100 kW) are being investigated. The power supply for these missions may require other than solar power; nuclear sources need to be considered.

As an illustration of the benefit in applying electric propulsion, consider a typical geosynchronous communications satellite with a 15-year lifetime and

with a mass of 2600 kg. For north-south station-keeping (NSSK) the satellite might need an annual velocity increase of some 50 m/sec; this requires about 750 kg of chemical propellant for the entire period, which is more than one-quarter of the satellite mass. Using an electric propulsion system can increase the specific impulse to 2800 sec (about nines times higher than a chemical rocket), and the propellant mass can be reduced to perhaps less than 100 kg. A power supply and electric thrusters would have to be added, but the inert mass of the chemical system can be deleted. Such an electric system would save perhaps 450 kg or about 18% of the satellite mass. At launch costs of \$30,000 per kilogram delivered to GEO, this is a potential saving of some \$13,500,000 per satellite. Alternatively, more propellant could be stored in the satellite, thus extending its useful life. Additional savings could materialize if electric propulsion were also used for orbit raising.

The power output (kinetic energy of jet per unit time, P or $P_{\rm jet}$) is really the basic energy rate supplied by the power source, principally diminished by (1) the losses of the power conversion, such as from solar into electrical energy; (2) conversion into the forms of electric energy suitable for the thrusters; and (3) the losses of the conversion of electric energy into propulsive jet energy. The kinetic power of the jet P per unit thrust F can be expressed by the simple relation (assuming no significant pressure thrust)

$$P/F = \frac{1}{2}\dot{m}v^2/\dot{m}v = \frac{1}{2}v = \frac{1}{2}g_0I_s \tag{19-1}$$

where \dot{m} is the mass flow rate, v the average jet discharge velocity (v_2 or c in Chapters 2 and 3), and I_s the specific impulse. The power-to-thrust ratio of the jet is therefore proportional to the exhaust velocity or the specific impulse. Thus, electrical propulsion units with very substantial values of I_s require more power per unit of thrust and incidentally a more massive power supply.

Thruster efficiency η_t is defined as the ratio of the thrust-producing kinetic energy (axial component) rate of the exhaust beam to the total electrical power supplied to the thruster, including any used in evaporating or ionizing the propellant, or

$$\eta_t = \frac{\text{power of the jet}}{\text{electrical power input}} = \frac{P_{\text{jet}}}{\Sigma(IV)}$$
(19–2)

Then, from the fundamentals in Chapter 2 (Eqs. 2-19 and 2-22),

$$\eta_t = \frac{\frac{1}{2}\dot{m}v^2}{P_e} = \frac{FI_s \ g_0}{2P_e} = \frac{FI_s \ g_0}{2\Sigma(IV)}$$
(19–3)

with P_e the electric power input to the thruster in watts, usually the product of the electrical current and all associated voltages (hence the Σ -sign).

Thruster efficiency accounts for all the energy losses that do not result in kinetic energy, including (1) the wasted electrical power (stay currents, ohmic resistance, etc.); (2) unaffected or improperly activated propellant particles (propellant utilization); (3) loss of thrust resulting from dispersion of the exhaust (direction and magnitude); and (4) heat losses. It is a measure of how effectively electric power and propellant are used in the production of thrust.

When electrical energy is not the only input energy, Eq. 19–2 has to be modified; for example, the propellant may release energy (chemical monopropellant), as in hydrazine decomposition with a resistojet.

19.1. IDEAL FLIGHT PERFORMANCE

For the low thrust of electric propulsion with its relatively massive power generating systems, the flight regimes of space vehicles propelled by electric rockets are quite different from those using chemical rockets. Accelerations tend to be very low $(10^{-4} \text{ to } 10^{-6} g_0)$, thrusting times are typically long (several months), and spiral trajectories were originally suggested for spacecraft accelerated by these low thrusts. Figure 19–2 shows schemes for going from LEO to GEO including a spiral, a Hohman ellipse (see Section 4.5 on the *Hohman*

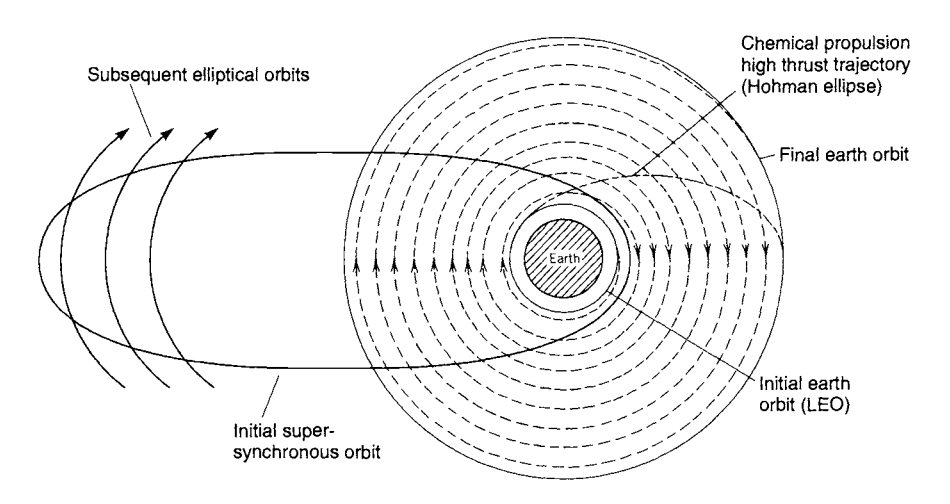


FIGURE 19–2. Simplified diagram of trajectories going from a low earth orbit (LEO) to a high earth orbit using chemical propulsion (short duration), electric propulsion with a multiple spiral trajectory (long duration), and a supersynchronous chemical orbit approach as an alternate to LEO (intermediate duration). From the supersynchronous orbit continuous thrusting with electric propulsion at a fixed inertial attitude lowers the apogee and raises the perigee in each orbit until it reaches the final high circular orbit. See Ref. 19–4.

orbit, which is optimum for chemical propulsion) as well as a "supersynchronous" orbit transfer (Ref. 19–4). Because of the long transfer orbit durations, trajectories other than spiral are presently being considered where one utilizes chemical propulsion to arrive at a very eccentric, supersynchronous elliptical orbit; from there electric propulsion can continuously and effectively be fired to attain a GEO orbit.

The performance of an electrical rocket can be conveniently analyzed in terms of the power and the relevant masses (Ref. 19–5). Let m_0 be the total initial mass of the vehicle stage, m_p the total mass of the propellant to be expelled, m_{pl} the payload mass to be carried by the particular stage under consideration, and m_{pp} the mass of the power plant consisting of the empty propulsion system including the thruster, propellant storage and feed system, the energy source with its conversion system and auxiliaries, and the associated structure. Then

$$m_0 = m_p + m_{pl} + m_{pp} ag{19-4}$$

The energy source input to the power supply (i.e., solar or nuclear) has to be larger than its electrical power output; they are related by the power conversion efficiency (about 10 to 15% for photovoltaic and up to 30% for rotating machinery) for converting the raw energy into electrical power at the desired voltages, frequencies, and power levels. The converted electrical output P_e is then supplied to the propulsion system. The ratio of the electrical power P_e to the mass of the power plant m_{pp} is defined as α , which is often referred to as the specific power of the power plant or of the entire propulsion system. This specific power must be defined for each design, because even for the same type of engine, α is somewhat dependent on the engine–module configuration (this includes the number of engines that share the same power conditioner, redundancies, valving, etc.):

$$\alpha = P_e/m_{pp} \tag{19-5}$$

The specific power is considered to be proportional to engine-power and reasonably independent of m_p . Its value hinges on technological advances and the electric-propulsion engine module configuration. Presently, typical values of α range between 100 and 200 W/kg. In the future it is hoped that α will attain values of 500 to 2000 W/kg pending some breakthrough in power conditioning equipment. Electrical power is converted by the thruster into kinetic energy of the exhaust. Allowing for losses by using the thruster efficiency η_t , defined in Eqs. 19–2 and 19–3, the electric power input is

$$P_e = \alpha m_{pp} = \frac{1}{2} \dot{m} v^2 / \eta_t = m_p v^2 / (2t_p \eta_t)$$
 (19–6)

where m_p is the propellant mass, v the effective exhaust velocity, and t_p the time of operation or propulsive time when the propellant is being ejected at a uniform rate.

Using Eqs. 19-4, 19-5, and 19-6 together with 4-7, one can obtain a relation for the reciprocal payload mass fraction (see Problem 19-4)

$$\frac{m_0}{m_{pl}} = \frac{e^{\Delta u/v}}{1 - (e^{\Delta u/v} - 1)v^2/(2\alpha t_p \eta_t)}$$
(19–7)

This assumes a gravity-free and drag-free flight. The change of vehicle velocity Δu which results from the propellant being exhausted at a speed v is plotted in Fig. 19–3 as a function of propellant mass fraction. The specific power α and the thruster efficiency η_t as well as the propulsive time t_p can be combined into a *characteristic speed* (Ref. 19–5)

$$v_c = \sqrt{2\alpha \ t_p \eta_t} \tag{19-8}$$

This characteristic speed is not a physical speed but rather a defined grouping of parameters that has units of speed; it can be visualized as the speed the power plant would have if its full power output were converted into the form of kinetic energy of its own inert mass m_{pp} . Equation 19–8 includes the propulsive time t_p which is the actual mission time (certainly, mission time cannot be smaller than the thrusting time). From Fig. 19–3 it can be seen that, for a given payload fraction (m_{pl}/m_0) and characteristic speed (v_c) , there is an opti-

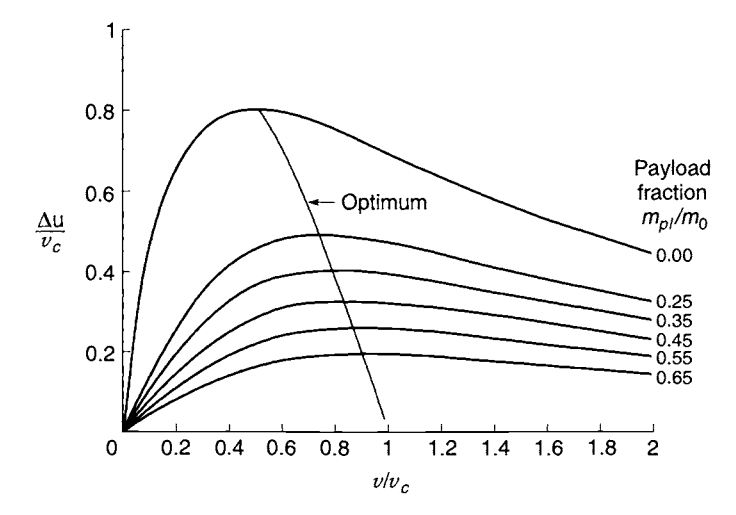


FIGURE 19–3. Normalized vehicle velocity increment as a function of normalized exhaust velocity for various payload fractions with zero inert mass of the propellant tank. The optima of each curve are connected by a line that represents Eq. 19–9.

mum value of v corresponding to the peak vehicle velocity increment; this is later shown to signify that there exists a particular set of most desirable operating conditions.

The peak for the curves in Fig. 19-3 exists because the inert mass of the power plant m_{pp} increases with the specific impulse while the propellant mass decreases with specific impulse. For a constant flow rate, other components are fixed in mass so that they only displace the curves by a constant amount. As indicated in Chapter 17 and elsewhere, this trend is generally true for all propulsion systems and leads to the statement that, for a given mission, there is theoretically an optimum range of specific impulse and thus an optimum propulsion system design. The peak of each curve in Fig. 19-3 is nicely bracketed by the ranges $\Delta u/v_c \le 0.805$ and $0.505 \le v/v_c \le 1.0$. This means that for any given electric engine any optimum operating time t_p^* will be proportional to the square of the total required change in vehicle velocity and thus large Δu 's would correspond to very long mission times. Similarly, any optimum specific impulse I_s^* will be (nearly) proportional to the change in vehicle velocity and large changes here would necessitate correspondingly high specific impulses. These conclusions will be refined in Section 19.4.

The optimum of the curves in Fig. 19–3 can be found by differentiating Eq. 19–7

$$\left(\frac{v}{\Delta u}\right) \left(e^{\Delta u/v} - 1\right) - \frac{1}{2} \left(\frac{v_c}{v}\right)^2 - \frac{1}{2} = 0 \tag{19-9}$$

This relates Δu , v, and v_c for maximum payload fraction (see Ref. 19-1).

All the equations quoted so far apply to all three fundamental types of electric rocket systems. No engine parameters are necessary except for the overall efficiency, which ranges from 0.4 to 0.8 in well-designed electric propulsion units, and α , which varies more broadly.

The problem with the above formulation is that the equations are underconstrained in that, given a velocity increment, mission time and specific impulse can be independently assigned. We will return to this topic in Section 19.4.

Example 19–1. Determine the flight characteristics of an electrical propulsion rocket for raising a low satellite orbit. Data given:

$$I_s = 2000 \text{ sec}$$

 $F = 0.20 \text{ N}$
Duration = 4 weeks = $2.42 \times 10^6 \text{ sec}$
Payload mass = 100 kg
 $\alpha = 100 \text{ W/kg}$
 $\eta_t = 0.5$

SOLUTION. The propellant flow is, from Eq. 2-13,

$$\dot{m} = F/(I_s g_0) = 0.2/(2000 \times 9.81) = 1.02 \times 10^{-5} \text{kg/sec}$$

The total required propellant is

$$m_p = \dot{m}t = 1.02 \times 10^{-5} \times 2.42 \times 10^6 = 24.69 \text{ kg}$$

The required electrical power is, from Eq. 19-6,

$$P_e = \frac{1}{2}\dot{m}v^2/\eta_t = \frac{1}{2}(1.02 \times 10^{-5} \times 2000^2 \times 9.81^2)/0.5 = 3.92 \,\text{kW}$$

The mass of the propulsion system and energy supply system is, from Eq. 19–5,

$$m_{pp} = P_e/\alpha = 3.92/0.1 = 39.2 \text{ kg}$$

The mass before and after engine operation (see Eq. 19-4) is

$$m_1 = 100 + 24.7 + 39.2 = 163.9 \text{ kg}$$

 $m_2 = 139.2 \text{ kg}$

The velocity increase of the stage under ideal vacuum and zero-g conditions (Eq. 4-6) is

$$\Delta u = v \ln[m_0/(m_0 - m_p)]$$

= 2000 × 9.8 \ln(163.9/139.2) = 3200 \text{ m/sec}

The average acceleration of the vehicle is

$$a = \Delta u/t = 3200/2.42 \times 10^6 = 1.32 \times 10^{-3} \text{m/sec}^2$$

= 1.35 × 10⁻⁴g₀

The flight's energy increase after 4 weeks of continuous thrust-producing operation is not enough to get from LEO to GEO (which would have required a change of vehicle velocity of about 4700 m/sec with continuous low thrust). During its travel the satellite will have made about 158 revolutions around the earth and raised the orbit by about 13,000 km. Moreover, this does not represent an optimum. In order to satisfy Eq. 19–9 it would be necessary to increase the burn duration (operating time) or change the thrust, or both.

19.2. ELECTROTHERMAL THRUSTERS

In this category, the electric energy is used to heat the propellant, which is then thermodynamically expanded through a nozzle. There are two basic types in use today:

- 1. The *resistojet*, in which components with high electrical resistance dissipate power and in turn heat the propellant, largely by convection.
- 2. The *arcjet*, in which current flows through the bulk of the propellant gas which has been ionized in an electrical discharge. Being relatively devoid of material limitations, this method introduces more heat directly into the gas (it can reach local temperatures of 20,000 K or more). The electrothermal arcjet is a unit where magnetic fields (either external or self-induced by the current) are not as essential for producing thrust as is the nozzle. As shown in Section 19.4, arcjets can also operate as electromagnetic thrusters, but here the magnetic fields are essential for acceleration and propellant densities are much lower. Thus, there are some arc-thruster configurations that could be classified as both electrothermal and electromagnetic.

Resistojets

These devices are the simplest type of electrical thruster because the technology is based on conventional conduction, convection, and radiation heat exchange. The propellant is heated by flowing over an ohmically heated refractory-metal surface, such as (1) coils of heated wire, (2) through heated hollow tubes, (3) over heated knife blades, and (4) over heated cyclinders. Power requirements range between 1 W and several kilowatts; a broad range of terminal voltages, AC or DC, can be designed for, and there are no special requirements for power conditioning. Thrust can be steady or intermittent as programmed in the propellant flow.

Material limitations presently cap the operating temperatures to under 2700 K, yielding maximum specific impulses of about 300 sec. The highest specific impulse has been achieved with hydrogen (because of its lowest molecular mass), but its low density causes propellant storage to be bulky (cryogenic storage being unrealistic for space missions). Since virtually any propellant is appropriate, a large variety of different gases has been used, such as O₂, H₂O, CO₂, NH₃, CH₄, and N₂. Also, hot gases resulting from the catalytic decomposition of hydrazine (which produces approximately 1 volume of NH₃ and 2 volumes of H₂ [see Chapter 7]) have been successfully operated. The system using liquid hydrazine (Ref. 19-6) has the advantage of being compact and the catalytic decomposition preheats the mixed gases to about 700°C (1400°F) prior to their being heated electrically to an even higher temperature; this reduces the required electric power while taking advantage of a well-proven space chemical propulsion concept. Figure 19–4 shows details of such a hybrid resistojet which is fed downstream from a catalyst bed where hydrazine is decomposed into hot gases.

Resistojets have been proposed for manned long-duration deep space missions, where the spacecraft's waste products (e.g., H₂O or CO₂) could then be

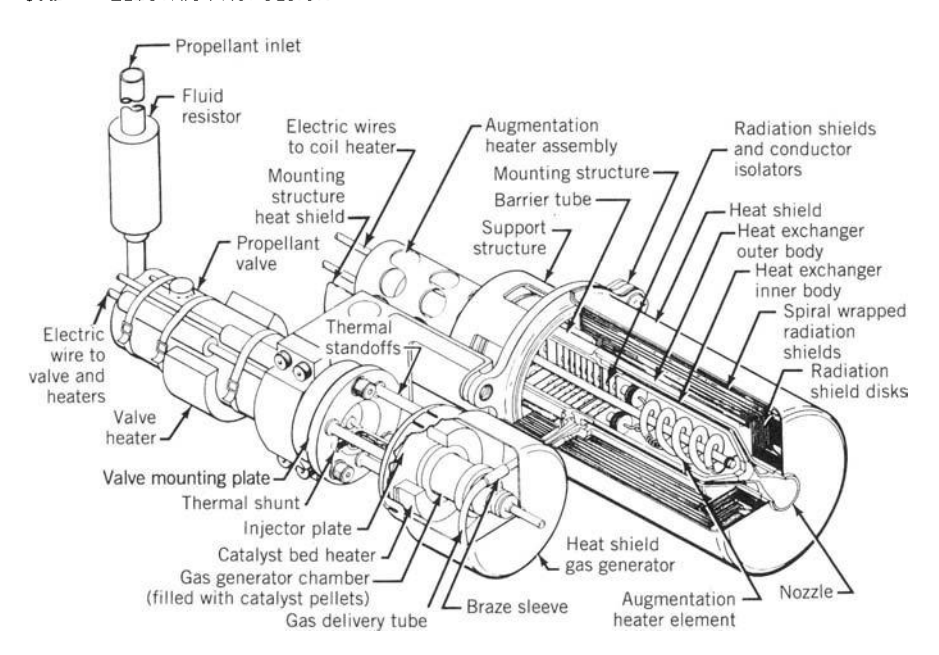


FIGURE 19-4. Resistojet augmented by hot gas from catalytically decomposed hydrazine; two main assemblies are present: (1) a small catalyst bed with its electromagnetically operated propellant valve and heaters to prevent hydrazine from freezing, and (2) an electrical resistance spiral-shaped heater surrounded by thin radiation shields, a refractory metal exhaust nozzle, and high-temperature electrical insulation supporting the power leads. (Courtesy of PRIMEX Aerospace Company.)

used as propellants. Unlike the ion engine and the Hall thruster, the same resistojet design can be used with different propellants.

In common with nearly all electric propulsion systems, resistojets have a propellant feed system that has to supply either gas from high-pressure storage tank or liquid under zero gravity conditions. Liquids require positive tank expulsion mechanisms, which are discussed in Chapter 6, and pure hydrazine needs heaters to keep it from freezing.

Engineering considerations in the development of these rockets include intermittent heat transfer from the heating element to the propellant, conduction and radiation losses from the chamber, the capability of materials to withstand the hot environment, and the heat capacity of the propellant. Procedures have been developed to account for specific heat, thermal conductivity, dissociation, and gas density variations with temperature. The gas flow in the heating chamber is typically considered to be either laminar or vortex flow, and the heat transfer to the stream is by convection.

Available materials limit the maximum gas temperature of a resistojet. High-temperature materials used for the resistance element include rhenium and refractory metals and their alloys (e.g., tungsten, tantalum, molybdenum),

platinum (stabilized with yttrium and zirconia), as well as cermets. For high-temperature electrical (but not thermal) insulation, boron nitride has been used effectively.

A design objective is to keep heat losses in the chamber at a low level relative to the power consumed. This can be done by (1) the use of external insulation, (2) internally located radiation shields, and (3) entrant flow layers or cascades. Within reason, the mass of insulation and radiation shields should be small compared to that of the thruster and of the total propulsion system.

The choice of chamber pressure is influenced by several factors. High pressures reduce molecular gas dissociation losses in the chamber, increase the rate of recombination in the exhaust nozzle, improve the heat exchanger performance, and reduce the size of both the chamber and the nozzle for a given mass flow rate. However, high pressures cause higher heat transfer losses, higher stresses on the chamber walls, and can accelerate the rate of nozzle throat erosion. The lifetime of a resistojet is often dictated by the nozzle throat life. Good design practice, admittedly a compromise, sets the chamber pressure in the range of 15 to 200 psi.

Thruster efficiencies of resistojets range between 65 and 85%, depending on the propellant and the exhaust gas temperature, among other things. The specific impulse delivered by any given electrothermal design depends primarily on (1) the molecular mass of the propellant, and (2) the maximum temperature that the chamber and the nozzle surfaces can tolerate.

Table 19–3 gives typical performance values for a resistojet augmented by chemical energy release. The specific impulse and thrust increase as the electric power of the heater is increased. An increase in flow rate (at constant specific power) results in an actual decrease in performance. The highest specific power (power over mass flow rate) is achieved at relatively low flow rates, low thrusts, and modest heater augmentation. At the higher temperatures the dissociation of molecular gases noticeably reduces the energy that is available for thermodynamic expansion.

Even with its comparatively lower value of specific impulse, the resistojet's superior efficiency contributes to far higher values of thrust/power than any of its nearest competitors. Additionally, these engines possess the lowest overall system empty mass since they do not require a power processor and their plumes are uncharged (thus avoiding the additional equipment that ion engines require). Resistojets have been recently employed in Intelsat V, Satcom 1-R, GOMS, Meteor 3-1, Gstar-3, and Iridium spacecraft. They are most attractive for low to modest levels of mission velocity increments, where power limits, thrusting times, and plume effects are mission drivers.

Arcjets

The basic elements of an arcjet thruster are shown in Fig. 1–8 where the relative simplicity of the physical design masks its rather complicated phenomenology. The arcjet overcomes the gas temperature limitations of the resistojet by the use

TABLE 19–3. Selected Performance Values of a Typical Resistojet with Augmentation

Propellant for resistojet	Hydrazine liquid, decomposed	
	by catalysis	
Inlet pressure (MPa)	0.689-2.41	
Catalyst outlet temperature (K)	1144	
Resistojet outlet temperature (K)	1922	
Thrust (N)	0.18-0.33	
Flow rate (kg/sec)	$5.9 \times 10^{-5} - 1.3 \times 10^{-4}$	
Specific impulse in vacuum (sec)	280-304	
Power for heater (W)	350-510	
Power for valve (max.) (W)	9	
Thruster mass (kg)	0.816	
Total impulse (N-sec)	311,000	
Number of pulses	500,000	
Minimum off-pulse bit (N-sec)	0.002	
Status	Operational	

Source: Data sheet for model MR-501, Primex Aerospace Company.

of an electric arc for direct heating of the propellant stream to temperatures much higher than the wall temperatures. The arc stretches between the tip of a central cathode and an anode, which is part of the coaxial nozzle that accelerates the heated propellant. These electrodes must be electrically insulated from each other and be able to withstand high temperatures. At the nozzle it is desirable for the arc to attach itself as a diffuse annulus in the divergent portion just downstream of the throat. The region of attachment is known to move up or down depending on the magnitude of the arc voltage and on the mass flow rate. In reality, arcs are highly filamentary and tend to heat only a small portion of the flowing gas unless the throat dimension is sufficiently small; bulk heating is done by mixing, often with the aid of vortex flow and turbulence. Since not all the heat is released prior to expansion in the nozzle, there is some loss in that heat released in the divergent portion of the nozzle is not effective in increasing the Mach number of the flow velocity in the exit divergent section.

Arcs are inherently unstable, often forming pinches and wiggles; they can be somewhat stabilized by an external electric field or by swirling vortex motion in the outer layers of the gas flow. The flow structure at the nozzle throat is quite nonuniform and arc instabilities and erosion at the throat are very limiting. The mixing of cooler outer gas with the arc-heated inner gas tends to stabilize the arc while lowering its conductivity, which in turn requires higher voltages of operation. In some designs the arc is made longer by lengthening the throat.

The analysis of arcjets is based on plasma physics, as it applies to a moving ionized fluid. The conduction of electricity through a gas requires that a certain

level of ionization be present. This ionization must be obtained from an electrical discharge, i.e., the breakdown of the cold propellant resembling a lightning discharge in the atmosphere (but, unlike lightning, a power supply may feed the current in a continuous or pulsed fashion). Gaseous conductors of electricity follow a modified version of Ohm's law. In an ordinary uniform medium where an electrical current I is flowing across an area A through a distance d by virtue of a voltage drop V, we can write Ohm's law as

$$V = IR = (I/A)(AR/d)(d)$$
 (19–10)

As given, the medium is uniform and thus we may define the electric field as E = V/d, the current density as j = I/A, and we introduce the *electrical conductivity* as $\sigma = d/AR$. We can now rewrite the basic Ohm's law as simply $j = \sigma E$. The scalar electrical conductivity is directly proportional to the density of unattached or *free electrons* that, under equilibrium, may be found from Saha's equation (Ref. 19–7). Strictly speaking, Saha's equation applies to thermal ionization only (and not necessarily to electrical discharges). For most gases, either high temperatures or low ionization energies or both are required for plentiful ionization. However, since only about one in a million electrons is sufficient for good conductivity, an inert gas can be seeded with alkali-metal vapors, as is amply demonstrated in plasmas for power generation. The value of plasma electrical conductivity σ may be calculated from

$$\sigma = e^2 n_e \tau / \mu_e \tag{19-11}$$

Here e is the electron charge, n_e the electron number density, τ the mean time between collisions, and μ_e the electron mass.

Actually, arc currents are nearly always influenced by magnetic fields, external or self-induced, and a *generalized Ohm's law* (Ref. 19–8) in a moving gas is needed such as the following vector form (this equation is given in scalar forms in the section on electromagnetic devices):

$$j = \sigma[\mathbf{E} + \mathbf{v} \times \mathbf{B} - (\beta/\sigma B)(\mathbf{j} \times \mathbf{B})]$$
 (19–12)

The motion of the gas containing charged particles is represented by the velocity v; the magnetic induction field is given as B (a scalar B in the above equation is required in the last term) and the electric field as E. In Eq. 19-12, both the current density j and the conductivity are understood to relate to the free electrons as does β , the Hall parameter. This Hall parameter is made up from the electron cyclotron frequency (ω) multiplied by the mean time it takes an electron to lose its momentum by collisions with the heavier particles (τ). The second term in Eq. 19-12 is the induced electric field due to the motion of the plasma normal to the magnetic field, and the last term represents the Hall electric field which is perpendicular to both the current vector and the applied magnetic field vector as the crossproduct (i.e., the "×") implies (ionslip and the electron pressure gradient have been omitted above, for simplicity).

Magnetic fields are responsible for most of the peculiarities observed in arc behavior, such as pinching (a constriction arising from the current interacting with its own magnetic field), and play a central role in non-thermal electromagnetic forms of thrusting, as discussed in a following section.

Analytical descriptions of arcjets, based on the configuration shown in Fig. 19–5, may include the following:

- 1. The energy input occurs largely in the small-diameter laminar flow arc region within the throat of the nozzle. As a first approximation, the power can be computed from Joule heating $[j \cdot E]$; here the current density and the voltage gradient across the arc have to be determined.
- 2. The cathode tip needs to be hot for thermionic emission of the arc electrons. It is heated by the arc and cooled by the propellant flow. The cathode, typically a coaxial pointed rod, is located in the plenum region.
- 3. The nozzle inner walls are heated by the arc, which may be at a temperature of 10,000 to 20,000 K. Typically the nozzle is cooled only by conduction and by the boundary layers.
- 4. The hot gas in the arc proper must mix quickly with the rest of the propellant; this is done by vortexing and turbulence.
- 5. Portions of the anode are heated to extreme temperatures in a section of the divergent nozzle at the arc footpoint (the arc attachment region of the electrode). The heating of the propellant is not all contained in the plenum chamber, and heating of a supersonic flow is a source of losses.

To start an arcjet, a much higher voltage than necessary for operation has to be applied momentarily in order to break down the cold gas. Some arcjets require an extended initial burn-in period before stable consistent running ensues. Because the conduction of electricity through a gas is inherently unstable, arcs require an external ballast resistance to allow steady-state operation. The cathode must run hot and is usually made of tungsten with 1 or 2% thorium (suitable up to about 3000 K). Boron nitride, an easily shaped high-temperature electrical insulator, is commonly used. Carbon sheets are often used between flanges.

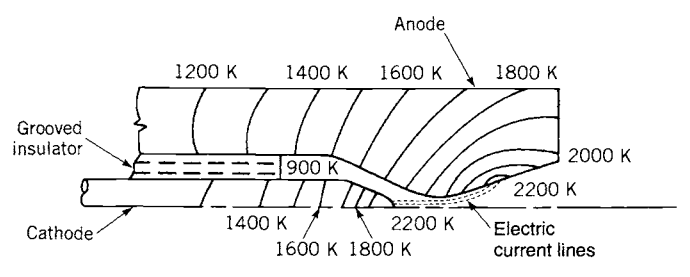


FIGURE 19-5. Typical estimated temperature distribution in the electrodes of an arcjet.

Presently, most arcjets are rather inefficient since less than half of the electrical energy goes into kinetic energy of the jet; the nonkinetic part of the exhaust plume (residual internal energy and ionization) is the largest loss. About 10 to 20% of the electric power input is usually dissipated and radiated as heat to space or transferred by conduction from the hot nozzle to other parts of the system. Arcjets, however, are potentially more scalable to large thrust levels than other electric propulsion systems. Generally, arcjets exhibit about six times the thrust-to-power ratio of a resistojet because of their increased specific impulse coupled with relatively low values of efficiency. Arcjets have another disadvantage in that the required power processing units are somewhat more complex than those for resistojets, due to the complexity of arc phenomena.

The life of an arcjet can be severely limited by local electrode erosion and vaporization, which is specifically due to action of the arc attachment point and of the high operating temperatures in general. The rate of erosion is influenced by the particular propellant in combination with the electrode materials (argon and nitrogen give higher erosion rates than hydrogen), and by pressure gradients, which are usually higher during start or pulsing transients (sometimes by a factor of 100) than during steady-state operation. A variety of propellants has been used in arcjet devices, including N₂, He, H₂, Ne, NH₃, Ar, and the catalytic decomposition products of N₂H₄. Lithium metal, which is a liquid at 180°C, has been considered because of its low molecular mass, ease of ionization, and its potential for transpiration cooling. Also lithium deposits on the cathode tend to reduce cathode erosion. Lithium is very reactive and requires special handling. Specific impulses for H₂ are 1200 to 1500 sec, which, along with other desirable heat-transfer properties, make both hydrogen and lithium the propellants of choice for high performance. There are, however, problems in the handling and storage of these propellants that have been difficult to resolve.

An arcjet downstream of a catalytic hydrazine decomposition chamber looks similar to the resistojet of Fig. 19–4, except that the resistor is replaced by a smaller diameter arc heater. Also, larger cabling is needed to supply the relatively much larger currents. Decomposed hydrazine would enter the arc at a temperature of about 760°C. Liquid hydrazine is easier to store and provides a low-volume, lighter-weight propellant supply system when compared to gaseous propellants. Table 19–4 shows on-orbit performance of a system of 2-kW hydrazine arcjets. Specific impulses from 400 to nearly 600 sec are typical for hydrazine arcjets (Ref. 19–9). A 26-kW ammonia arcjet program (ESEX) is presently undergoing space testing (Refs. 19–10, 19–11) with 787 sec specific impulse and 1.93 N thrust.

19.3. NON-THERMAL ELECTRICAL THRUSTERS

The acceleration of a hot propellant through the use of a supersonic nozzle is the most conspicuous feature of thermal thrusting. Now we turn our study to

TABLE 19-4. On-Orbit 2 kW Hydrazine Arcjet System (PRIMEX, Ref. 19-9)

Propellant	Hydrazine
Steady thrust	222-258 mN
Mass flow rate	36-47 mg/sec
Feed pressure	185–330 psia
Power control unit (PCU) input	4.4 kW (two thrusters)
System input voltage	68–71 V DC
PCU efficiency	93%
Specific impulse	570-600 sec
Dimensions	
Arcjet	$237 \times 125 \times 91 \text{ mm}^3$
PCU	$632 \times 361 \times 109 \text{ mm}^3$
Mass	
Arcjet (4) and cable	6.3 kg
PCU	15.8 kg
Total impulse	1,450,000 N-sec

acceleration of a propellant by electrical forces where no area changes are essential for direct gas acceleration. The electrostatic (or Coulomb) force and the electromagnetic (or Lorentz) force can be used to accelerate a suitable propellant to speeds ultimately limited by the speed of light (note that thermal thrusting is essentially limited by the speed of sound in the plenum chamber). The microscopic vector force \mathbf{f}_e on a *singly charged particle* can be written as

$$f_e = e\mathbf{E} + e\mathbf{v}_e \times \mathbf{B} \tag{19-13}$$

where e is the electron charge magnitude, E the electric field vector, v_e the velocity of the charged particle, and B the magnetic field vector. The sum of the electromagnetic forces on all the charges gives the total force per unit volume vector \tilde{F}_e (scalar forms of this equation follow)

$$\tilde{\mathbf{F}}_{e} = \rho_{e}\mathbf{E} + \mathbf{i} \times \mathbf{B} \tag{19-14}$$

Here ρ_e is the *net charge density* and j the electric current vector density. With plasmas, which by definition have an equal mixture of positively and negatively charged particles within a volume of interest, this net charge density vanishes. On the other hand, the current due to an electric field does not vanish because positive ions move opposite to electrons, thus adding to the current (but in plasmas with free electrons this ion current can be very small). From Eq. 19–14, we see that an electrostatic accelerator must have a nonzero net charge density that is commonly referred to as a *space-charge density*. An example of an electrostatic accelerator is the ion engine, which operates with positive ions; here magnetic fields are unimportant in the accelerator region. Electromagnetic accelerators operate only with plasmas and rely solely on the Lorentz force to

accelerate the propellant. The Hall accelerator may be thought of as a crosslink between an ion engine and an electromagnetic engine. These three types of accelerator are discussed next. Research and development efforts in the field of non-thermal thrusters have been extensive and truly international.

Electrostatic and electromagnetic devices require an understanding of the basic laws of electricity and magnetism which are most elegantly summarized in Maxwell's equations complemented by the force relation and Ohm's law, both previously introduced. Moreover, various processes in ionization and gaseous conduction need to be considered. This subject forms the basis of the discipline of magnetohydrodynamics or MHD; however, a proper treatment of this subject is beyond the scope of this book.

Electrostatic Devices

Electrostatic thrusters rely on Coulomb forces to accelerate a propellant composed of non-neutral charged particles. They can operate only in a near vacuum. The electric force depends only on the charge, and all charged particles must be of the same "sign" if they are to move in the same direction. Electrons are easy to produce and are readily accelerated, but they are so extremely light in mass as to be impractical for electric propulsion. From thermal propulsion fundamentals one might deduce that "the lighter the exhaust particle the better." However, the momentum carried by electrons is relatively negligible even at velocities near the speed of light. Thus, the thrust per unit area that can be imparted to such an electron flow remains negligible even when the effective exhaust velocity or specific impulse gets to be very high. Accordingly, electrostatic thrusters use charged heavy-molecular-mass atoms as positive ions (a proton is 1840 times heavier than the electron and a typical ion of interest contains hundreds of protons). There has been some research work with small liquid droplets or charged colloid which can in turn be some 10,000 times heavier than atomic particles. In terms of power sources and transmission equipment, the use of the heavier particles contributes to more desirable characteristics for electrostatic thrusters—for example, high voltages and low currents in contrast to low voltages and high currents with their associated massive wiring and switching.

Electrostatic thrusters can be categorized by their source of charged particles as follows:

- Electron bombardment thrusters. Positive ions from a monatomic gas are produced by bombarding the gas or vapor, such as xenon or mercury, with electrons emitted from a heated cathode. Ionization can be either DC or RF.
- 2. *Ion contact thrusters*. Positive ions are produced by passing the propellant vapor, usually cesium, through a hot (about 1100°C or 2000°F) porous tungsten contact ionizer. Cesium vapor was used extensively in the original ion engines.

3. Field emission or colloid thrusters. Tiny droplets of propellant are charged either positively or negatively as these droplets pass through an intense electric field discharge. The stability of large, charged particles remains a challenge.

Names such as xenon ion propulsion system (XIPS, Ref. 19–12, and NSTAR/DS1, Refs. 19–10 and 19–13), radio-frequency field ionization (RITA), cesium ion contact rockets, and colloid propulsion have been used to identify electrostatic thrusters. The following general design criteria are desirable for electrostatic thrusters, regardless of the charged particle source:

- 1. Minimum expenditure of energy per charged particle produced (this energy is an irrecoverable loss).
- 2. Minimum ion-collision damage to the accelerating electrodes (sputtering) and deterioration of component characteristics over thrust lifetime.
- 3. Maximum supply of ionized particles (related to propellant utilization factor).
- 4. Stabilized uniform operation near the space-charge limitations of the thruster (represented by the saturation current density within the accelerator electrodes).
- 5. Production of particles of uniform mass and charge so that they can be effectively accelerated by the electric field.
- 6. No reaction of the exhaust plume gases with spacecraft materials (Hg vapor can react with many materials).
- 7. Nonhazardous propellants with good tankage properties (Hg and Cs are poisonous and Xe is nontoxic but requires extra devices to conserve it). Good tankage means propellant of high density, that is noncorrosive, with stable storage over time.
- 8. No deposits of condensed species on spacecraft optical components (windows, lenses, mirrors, photovoltaic cell surfaces, or sensitive heat rejection surfaces).
- 9. Specific impulse near optimum for a given mission (the specific impulse is shown to be a function of accelerating voltage and the particle mass).

Basic Relationships for Electrostatic Thrusters

An electrostatic thruster, regardless of type, consists of the same series of basic ingredients, namely, a propellant source, several forms of electric power, an ionizing chamber, an accelerator region, and a means of neutralizing the exhaust. While Coulomb accelerators require a net charge density of one polarity, the exhaust beam must be neutralized to avoid a space-charge buildup outside of the craft which could easily nullify the operation of the thruster. Neutralization is achieved by the injection of electrons downstream (see the device descriptions that follow). The exhaust velocity is a function of the

voltage V_{acc} imposed across the accelerating chamber or grids, the mass of the charged particle μ , and its electrical charge e. In the conservation of energy equation the kinetic energy of a charged particle must equal the electrical energy gained in the field, provided that there are no collisional losses. In its simplest form,

$$\frac{1}{2}\mu v^2 = eV_{acc} {19-15}$$

Now, solving for the speed gained in the accelerator,

$$v = \sqrt{2eV_{acc}/\mu} \tag{19-16}$$

When e is in coulombs, μ in kilograms, and V_{acc} is in volts, then v is in meters per second. Using $\mathfrak M$ to represent the molecular mass of the ion ($\mathfrak M=1$ for a proton) then, for singly charged ions, the equation above becomes v (m/sec) = 13,800 $\sqrt{V_{acc}/\mathfrak M}$. References 19–2 and 19–3 contain a detailed treatment of the applicable theory.

In an ideal ion thruster, the current I across the accelerator represents the sum of all the propellant mass (100% singly ionized) carried per second by the particles accelerated:

$$I = \dot{m}(e/\mu) \tag{19-17}$$

The total ideal thrust from the accelerated particles is given by Eq. 2–14 (without the pressure thrust term, as pressures are extremely low):

$$F = \dot{m}v = I\sqrt{2\mu V_{acc}/e} \tag{19-18}$$

As can be seen, for a given current and accelerator voltage the thrust is proportional to the mass-to-charge ratio of the charged particles. The thrust and power absorbed by the neutralizing electrons are both small (about 1%) and can easily be neglected.

The current density *j* that can be obtained with a charged particle beam has a *saturation value* depending on the geometry and the electrical field (see Ref. 19–14). This fundamental limit is caused by the internal electric field associated with the ion cloud opposing the electric field from the accelerator when too many charges of the same sign try to pass simultaneously through the accelerator. The saturation current can be derived for a plane-geometry electrode configuration from basic principles. A definition of the current density in terms of the space charge density follows:

$$j = \rho_e v \tag{19-19}$$

The voltage in a one-dimensional space-charge region is found from Poisson's equation, where x represents distance and ε_0 is the *permittivity of free space* which, in SI units, has the value of 8.854×10^{-12} farads per meter:

$$d^2V/dx^2 = \rho_e/\varepsilon_0 \tag{19-20}$$

By solving Eqs. 19–16, 19–19, and 19–20 simultaneously and applying the proper boundary conditions, we obtain the following relation known as the *Child-Langmuir law*:

$$j = \frac{4\varepsilon_0}{9} \sqrt{\frac{2e}{\mu}} \frac{(V_{acc})^{3/2}}{d^2}$$
 (19–21)

In this equation, d is the accelerator interelectrode distance. In SI units the equation for the saturation current density can be expressed (for atomic or molecular ions) as

$$j = 5.44 \times 10^{-8} V_{acc}^{3/2} / (\mathfrak{M}^{1/2} d^2)$$
 (19–22)

Here the current density is in A/m^2 , the voltage is in volts, and the distance in meters. For xenon with electron bombardment schemes, values of j vary from 2 to about 10 mA/cm^2 . The current density and the area are very sensitive to the accelerator voltage as well as to the electrode configuration and spacing.

Using Eqs. 19–18 and 19–22 and letting the cross section be circular so that $I = (\pi D^2/4)j$, the thrust can be rewritten as

$$F = (2/9)\pi\varepsilon_0 D^2 V_{acc}^2 / d^2$$
 (19–23)

In SI units, for molecular ions, this becomes

$$F = 6.18 \times 10^{-12} V_{acc}^2 (D/d)^2$$
 (19–24)

The ratio of the exhaust beam emitter diameter D to the accelerator-electrode grid spacing d can be regarded as an aspect ratio of the ion accelerator region. For multiple grids with many holes (see Figs. 19–6 and 19–7) the diameter D is that of the individual perforation hole and the distance d is the mean spacing between grids. Because of space-charge limitations, D/d can have values no higher than about one for simple, single-ion beams. This implies a rather stubby engine design with many perforations and the need for multiple parallel ion engines for larger thrust values.

Using Eqs. 19–1, 19–2, and 19–17, and assuming η_t conversion of potential energy to kinetic energy, the power of the electrostatic accelerator region is

Gas	Ionization Potential (eV)	Molecular/Atomic Mass (kg/kg-mol)
Cesium vapor	3.9	132.9
Potassium vapor	4.3	39.2
Mercury vapor	10.4	200.59
Xenon	12.08	131.30
Krypton	14.0	83.80
Hydrogen, molecular	15.4	2.014
Argon	15.8	39.948
Neon	21.6	20.183

TABLE 19-5. Ionization Potentials for Various Gases

$$P_e = IV_{acc} = (1/2)\dot{m}v^2/\eta_t \tag{19-25}$$

The overall efficiency of an electrostatic thruster will be a function of the thruster efficiency η_t as well as of other loss factors. One loss of energy which is intrinsic to the thruster is the energy expended in charging the propellant, which is related to the ionization energy; it is similar to the dissociation energy in electrothermal devices. Ionization represents an input necessary to make the propellant respond to the electrostatic force and is non-recoverable. The ionization energy is found from the ionization potential (ε_t) of the atom or molecule times the current flow, as the example below shows. Historically, in the development of the ion engine, propellant charging has been of primary concern; the first engine designs used cesium because of its high vapor pressure and ease of ionization, but cesium has many undesirable tankage properties (its high reactivity is very difficult to isolate); then came mercury, with its wellknown ionization behavior from fluorescent lamps, but mercury also proved to be unworkable because of its poor tankage characteristics; finally, xenon emerged with its reliable tankage properties and its relative ease of ionization. Table 19–5 shows the molecular mass and first ionization potential for different propellants. In actual practice, considerably higher voltages than the ionization potential are required to operate the ionization chamber.

Example 19–2. For an electron-bombardment ion rocket the following data are given:

(131.3 kg/kg-mol)
l
1
V

Determine the thrust, exhaust velocity, specific impulse, mass flow rate, propellant needed for 91 days' operation, the power of the exhaust jets, and the thruster efficiency including ionization losses.

SOLUTION. The ideal thrust is obtained from Eq. 19-24:

$$F = 6.18 \times 10^{-12} \times (700)^2 \times (2/2.5)^2 = 1.94 \times 10^{-6} \text{ N per grid opening}$$

The total ideal thrust is then obtained by multiplying by the number of holes

$$F = 2200 \times 1.94 \times 10^{-6} = 4.26 \text{ milliN}$$

The exhaust velocity and specific impulse are obtained from Eq. 19-16:

$$v = 13,800\sqrt{700/131.3} = 31,860 \text{ m/sec}$$

 $I_s = 31,860/9.81 = 3248 \text{ sec}$

The mass flow rate, obtained from Eq. 2-6, is

$$\dot{m} = F/v = 4.26 \times 10^{-3}/31,860 = 1.34 \times 10^{-7} \text{ kg/sec}$$

For a cumulative period of 91 days of operation, the amount of xenon propellant needed (assuming no losses) is

$$m = \dot{m} t_p = 1.34 \times 10^{-7} \times 91 \times 24 \times 3600 = 1.05 \text{ kg}$$

The kinetic energy rate in the jet is

$$\frac{1}{2}\dot{m}v^2 = 0.5 \times 1.34 \times 10^{-7} \times (31,860)^2 = 67.9 \text{ W}$$

The ionization losses (l_1) represent the nonrecoverable ionization energy which is related to the ionization potential of the atom (ε_I) times the number of coulombs produced per second (see Table 19–5 and Eq. 19–17):

$$l_I = (12.08) \times (1.34 \times 10^{-7} \times 1.602 \times 10^{-19}) / (1.67 \times 10^{-27} \times 131.3) = 1.18 \text{ W}$$

As can be seen, the ionization energy in this ideal case is about 2% of the accelerator energy rate. An equivalent way of calculating the ionization energy is to multiply the ionization potential by the total ion current. The current is found from Eq. 19–17 to be just under 10 mA. Of course, other losses would detract from the high ideal efficiency of this device, which is 98.3%.

Ionization Schemes. Even though all ion acceleration schemes are the same, there are several ionization schemes for electrostatic engines. Most devices are DC but some are RF. To a great extent, the ionization chamber is responsible for most of the size, mass, and perhaps efficiency of these devices. We discuss some of these next.

Ionization of a gas by electron bombardment is a well-established technology (Ref. 19–14). Electrons are emitted from a thermionic (hot) cathode or the more efficient hollow cathode and are forced to interact with the gaseous propellant flow in a suitable ionization chamber. The chamber pressures are low, typically 10⁻³ torr or 0.134 Pa. Figure 19–6 depicts a typical electron-bombardment ionizer which contains neutral atoms, positive ions, and electrons. Emitted electrons are attracted toward the cylindrical anode but are forced by the axial magnetic field to spiral in the chamber, causing numerous collisions with propellant atoms which lead to ionization. A radial electric field removes the electrons from the chamber and an axial electric field moves the ions toward the accelerator grids. These grids act as porous electrodes, which

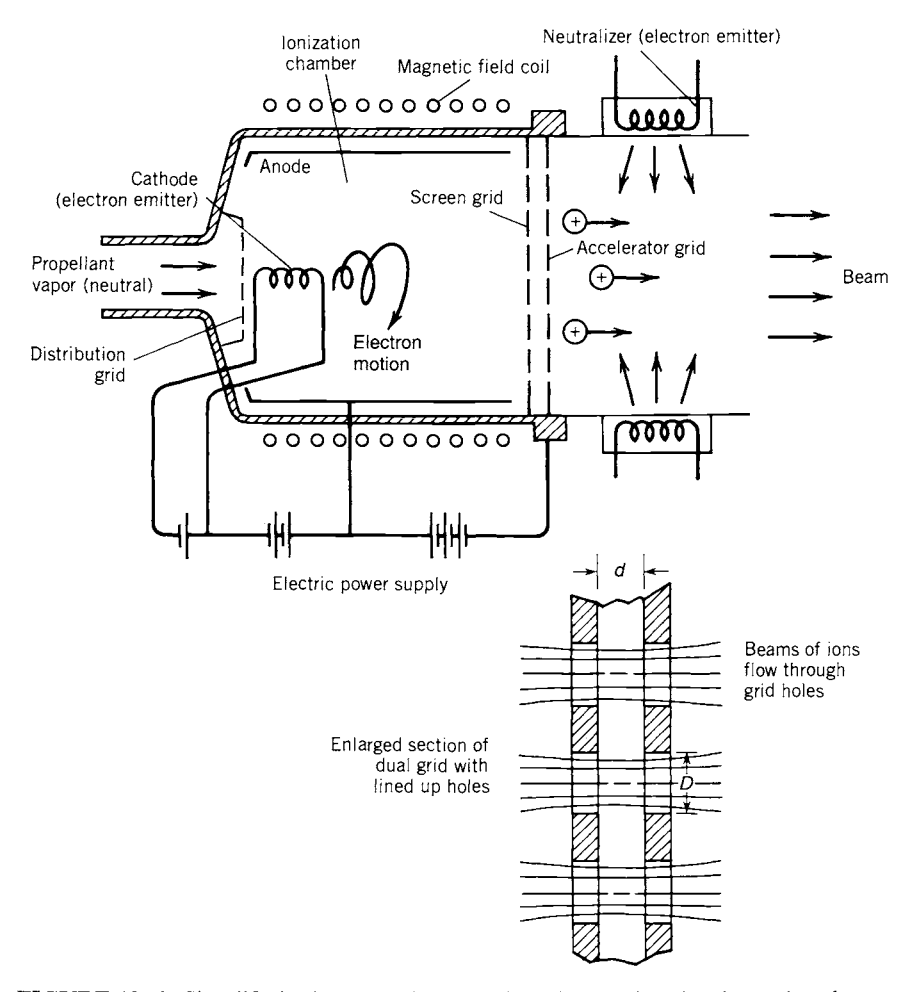


FIGURE 19–6. Simplified schematic diagram of an electron bombardment ion thruster, showing an enlarged section of the double grid.

electrostatically accelerate the positive ions. Loss of electrons is prevented by maintaining the cathode potential negatively biased on both the inner grid electrode and the opposite wall of the chamber. Electrons are routed from the cylindrical anode through an external circuit to another hot cathode at the exhaust beam in order to neutralize the exit beam.

Figure 19–7 shows a cross section of an ion propulsion thruster using xenon as a propellant. It has three perforated electrically charged grids: the inner one keeps the electrons in the ionizer, the middle one has a high voltage (1000 V or more) and accelerates the ions, and the outer one keeps the neutralizing electrons from entering the accelerator region. Each grid hole is lined up with a similar opening in the other grids and the ion beam flows through these holes. If the grids are properly designed, only a few ions are lost by collision with the surface; however, these collisions cause sputtering and greatly diminish the life of the grids. Heavy metals such as molybdenum have been used, with graphite composites being recently introduced. The neutralizer electron source is positioned outside the beam.

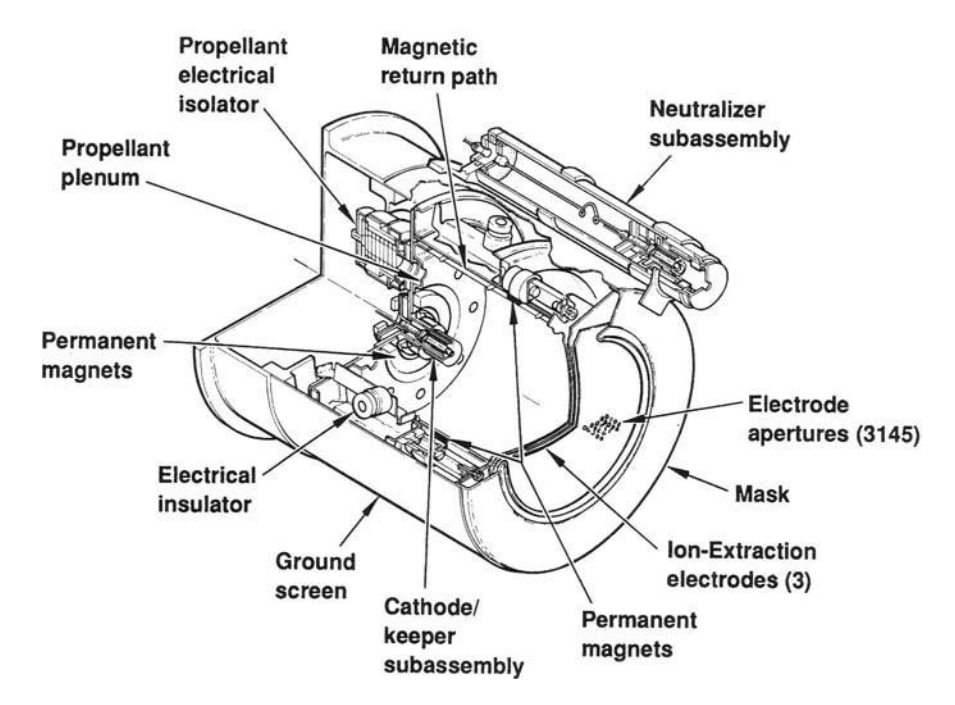


FIGURE 19–7. External view and section of a 500-watt ion propulsion system (XIPS), rated at 18 mN and 2800 sec. Permanent magnets are used on the outside of the ionization chamber; also shown are cathodes for ionization and for beam neutralization. Xenon gas is delivered to the ionizer, then accelerated through the three sheet electrodes, and then the ion beam is neutralized. (Drawing courtesy of Hughes Space and Communications and the American Physical Society.)

Other key components are (1) the heaters for the ionizer and neutralizer cathode, (2) propellant feed and electrical isolator, (3) electrical insulators, and (4) permanent magnets. Reference 19–12 describes a 500 W xenon thruster. Hollow cathodes represent an advancement in the state-of-the-art in electron emission; this cathode consists of a high-temperature metal tube with a flowlimiting orifice and a porous tungsten cylinder impregnated with a bariumoxygen compound located next to the orifice. At about 1370 K the cathode is a good thermionic emitter and thus the hot cylinder produces enough electrons at a relatively low temperature. Xenon, the stable inert gas with the highest molecular mass, is the propellant of choice. Xenon is a minor component of air, in a concentration of about 9 parts in 100 million, so it is a relatively rare and expensive propellant whose availability is currently limited. Its critical point is 289.7 K and 5.84 MPa (the critical density is 1100 kg/m³). It is easily stored below its critical temperature as a liquid and it does not pose any problems of condensation or toxicity. Pressure regulators for xenon need to be more sophisticated, because no leakages can be tolerated and because flows are very small.

In general, losses can be reduced by (1) decreasing the electron energy and ion density near the walls, (2) increasing the electron energy and ion density near the grid, and (3) optimizing the screen-grid open area. Practical limitations and trade-offs exist for each feature. For example, a reduction in electron energy to reduce the electron flux to the walls also increases collision losses. In practice a small portion of the accelerated ion current impinges on these grids, causing some power loss and some sputtering. Two aspects of the exhaust beam are non-thrust producing: one is the aforementioned ionization energy contained in the beam and the other one is any vector divergence present which results in beam spreading. Beam spreading, or the radial velocity component of beams, can result from causes both upstream and downstream of the exit electrode. Much of the divergence produced upstream is linked directly with internal geometrical details or "ion optics." Divergence downstream arises from forces within the beam or space charge spreading. Once outside of the accelerator chamber, repelling electrostatic forces between ions rapidly spread the beam radially. Proper neutralization of the beam reduces this spreading, allowing nearly axial velocities.

Other electrical charging schemes include surface or ion contact ionization, field emission ionization, and radio-frequency ionization. These are fairly compact and effective ionizers when compared to electron bombardment. In field emission charging, positive or negative particles are generated when tiny liquid droplets (colloids) pass through a corona discharge. The radio-frequency ion thruster consists of an RF electrodeless discharge that can be compact and produce a high specific impulse; work on this technology is being done primarily in Germany.

The *ion contact thruster* produces ions by surface ionization. The criterion that must be met is that the work function of the metal must be higher than the ionization potential of the propellant. As the propellant atoms "adsorb"

on the surface they lose their valence electron to the metal and are re-emitted as a positive ion. The requirement of a high work function and a hot metallic surface restricts this surface to the refractory metals, notably tungsten. Moreover, the requirement of low ionization potential and high atomic mass restricts the propellant to cesium. The operating principle is the same as in the so-called thermionic energy converter. Designs of the cesium/tungsten combination have not yielded high reliability over long lifetimes. Cesium as a propellant is extremely difficult to handle and has proven to be impractical for spacecraft.

Electromagnetic Thrusters

This third major type of electric propulsion device accelerates propellant gas that has been heated to a plasma state. Plasmas are mixtures of electrons, positive ions, and neutrals that readily conduct electricity at temperatures usually above 5000 K or 9000 R. According to electromagnetic theory, whenever a conductor carries a current perpendicular to a magnetic field, a body force is exerted on the conductor in a direction at right angles to both the current and the magnetic field. Unlike the ion engine, this acceleration process yields a neutral exhaust beam. Another advantage is the relatively high thrust density, or thrust per unit area, which is normally about 10 to 100 times that of the ion engines.

Many conceptual arrangements have undergone laboratory study, some with external and some with self-generated magnetic fields, some suited to continuous thrusting and some limited to pulsed thrusting. Table 19-6 shows ways in which electromagnetic thrusters can be categorized. There is a wide variety of devices with a correspondingly wide array of names. We will use the term Lorentz-force accelerators when referring to the principle of operation. For all of these devices the plasma is part of the current-carrying electrical circuit and most are accelerated without the need for area changes. Motion of the propellant, a moderate-density plasma or in some cases a combination of plasma and cooler gas particles, is due to a complex set of interactions. This is particularly true of short duration (3 to 10 µsec) pulsedplasma thrusters where nothing reaches an equilibrium state. Basically, the designer of an electromagnetic thruster tries to (1) create a body of electrically conductive gas, (2) establish a high current within by means of an applied electric field, and (3) accelerate the propellant to a high velocity in the thrust vector direction with a significantly intense magnetic field (often self-induced).

Conventional Thrusters—MPD and PPT. The description of magneto-plasma-dynamic (MPD) and pulsed-plasma (PPT) electromagnetic thrusters is based on the Faraday accelerator (Ref. 19-8). In its simplest form, a plasma conductor carries a current in the direction of an applied electric field but perpendicular to a magnetic field, with both of these vectors in turn normal to

Thrust Mode	Steady State	Pulsed (Transient)	
Magnetic field source	External coils or permanent magnets	Self-induced	
Electric current source	Direct-current supply	Capacitor bank and fast switches	
Working fluid	Pure gas, as mixture, seeded gas, or vaporized liquid	Pure gas or vaporized liquid or stored as solid	
Geometry of path of working fluid	Axisymmetric (coaxial) rectangular, cylindrical, constant or variable cross section	Ablating plug, axisymmetric, other	
Special features	Using Hall current or Faraday current	Simple requirement for propellant stage	

TABLE 19-6. Categories of Electromagnetic Thrusters

the direction of plasma acceleration. Equation 19–12 can be specialized to a Cartesian coordinate system where the plasma's "mass-mean velocity" is in the x-direction, the external electric field is in the y-direction, and the magnetic field acts in the z-direction. A simple manipulation of Eq. 19–12, with negligible Hall parameter β , yields a scalar equation for the current,

$$j_y = \sigma(E_y - v_x B_z) \tag{19-26}$$

and the Lorentz force becomes

$$\tilde{F}_x = j_y B_z = \sigma(E_y - v_x B_z) B_z = \sigma B_z^2 (E_y / B_z - v_x)$$
 (19–27)

Here \tilde{F}_x represents the force "density" within the accelerator and should not be confused with F the thrust force; \tilde{F}_x has units of force per unit volume (e.g., N/m³). The axial velocity v_x is a mass-mean velocity that increases internally along the accelerator length; the thrust equals the exit value (v_{max} or v_2) multiplied by the mass flow rate. It is noteworthy that, as long as E_y and B_z (or E/B) remain constant, both the current and the force decrease along the accelerator length due to the induced field $v_x B_z$ which subtracts from the impressed value E_y . This increase in plasma velocity translates into a diminishing force along such Faraday accelerators, which limits the final axial velocity. Although not practical it would seem desirable to design for increasing E/B along the channel in order to maintain a substantial accelerating force throughout. But it is not necessarily of interest to design for peak exit velocity because this might translate into unrealistic accelerator lengths (see Problem 19–8). It can be shown that practical considerations might restrict the exit velocity to below one-tenth of the maximum value of E_y/B_z .

A "gasdynamic approximation" (essentially an extension of the classical concepts of Chapter 3 to plasmas in an electromagnetic field) by Resler and Sears (Ref. 19–15) indicates that further complications are possible, namely, that a constant area accelerator channel would *choke* if the plasma velocity does not have the very specific value of [(k-1)/k](E/B) at the sonic location of the accelerator. This *plasma tunnel velocity* would have to be equal to 40% of the value of E/B for inert gases, since k (the ratio of specific heats) equals 1.67. Thus constant area, constant E/B accelerators could be severely constrained because Mach one corresponds only to about 1000 m/sec in typical inert gas plasmas. Constant-area choking in real systems, where the properties E, B, and σ are actually quite variable, is likely to manifest itself as one or more instabilities. Another problem is that values of the conductivity and electric field are usually difficult to determine and a combination of analysis and measurement is required to evaluate, for example, Eq. 19–12. Fortunately, most plasmas are reasonably good conductors when less than 10% of the particles are ionized.

Figure 19–8 shows the simplest plasma accelerator, employing a self-induced magnetic field. This is a *pulsed plasma thruster* (PPT), accelerating plasmas "struck" between two rail electrodes and fed by a capacitor, which is in turn charged by a power supply. The current flow through the plasma quickly discharges the capacitor and hence the mass flow rate must be pulsed according to the discharge schedule. The discharge current forms a current loop, which induces a strong magnetic field perpendicular to the plane of the rails. Analogous to a metal conductor in an electric motor, the Lorentz force acts on the plasma, accelerating it along the rails. For a rail width s, the *total internal accelerating force* has the value F = sIB, where I is the total current and B the magnitude of the self-induced field. Hence no area changes are required to accelerate the propellant. Some electrical energy is lost to the electrodes and the ionization energy is never recovered; moreover, this particular plasma does not exit well collimated, and propellant utilization tends to be poor.

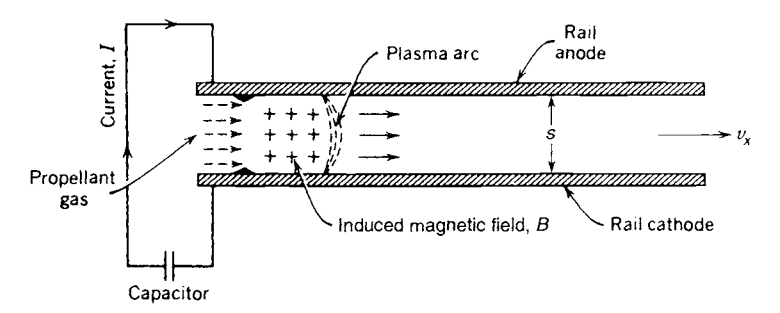


FIGURE 19–8. Simple rail accelerator for self-induced magnetic field acceleration of current-carrying plasma. The concept illustrates the basic physical interactions but suffers from loss of propellant, resulting in low efficiency.

A practical version of the PPT was first put in operation in 1968 and is shown in Chapter 1 as Fig. 1-10. It was used reliably in the USAF's LES-6 communication satellite, which had four PPTs producing approximately 12 million pulses over the life of the thruster. The propellant is stored in a solid Teflon bar that is pushed against the rails by a suitable spring. The rechargeable capacitor discharges across the Teflon surface, momentarily ablating it, and the current flow through the ionized vapor creates its own accelerating magnetic field. About 10⁻⁵ g of Teflon and 5000 A peak current flow during a 0.6 µsec pulse. In the LES-6 electric propulsion system, one-third of the energy is lost because of capacitor resistance. Other losses occur in ablation, dissociation, ionization, plasma and electrode heating. Teflon stores well in space, is easy to handle, and ablates with insignificant charring. In addition to the overall simplicity of the device, there are no tanks, valves, synchronizing controls, or zero-gravity feed problems. Another advantage is that pulsed thrusting is very compatible with precise control and positioning where the mean thrust is varied by changing the pulsing rate. Besides its very low efficiency, the big disadvantage of this thruster is the size and mass of the power conditioning equipment, which is presently the subject of technology programs toward improvement. Better PPTs are under development (Ref. 19–16).

Figure 19–9 shows a hybrid electrothermal—electromagnetic concept. It produces continuous thrust and Russians claim to have flown several versions. Compared to an electrothermal arcjet, these devices operate at relatively lower pressures and much higher electric and magnetic fields. Hydrogen and argon are common propellants for such MPD arcjets. As with other electromagnetic thrusters, exhaust beam neutralization is unnecessary. Problems of electrode

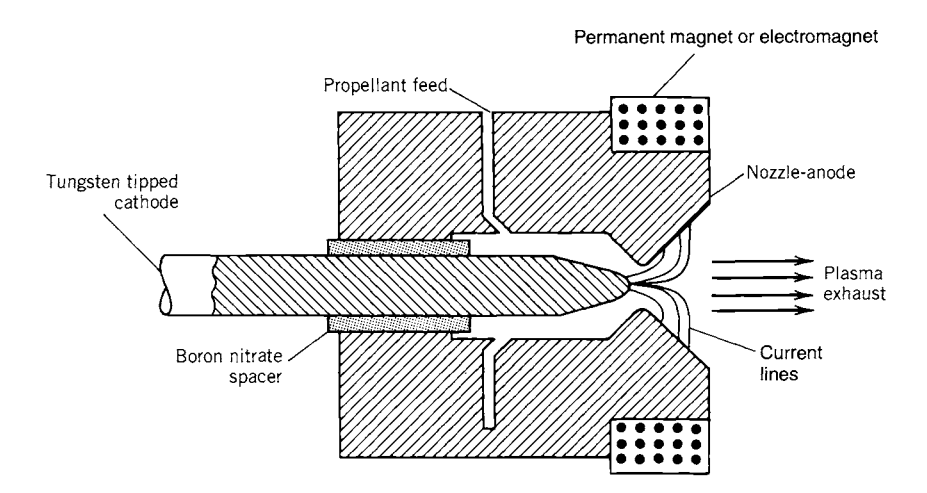


FIGURE 19-9. Simplified diagram of a magnetoplasma dynamic (MPD) arcjet thruster. It is similar in construction to the thermal arcjet shown in Fig. 1-8 but it has a stronger magnetic field to enhance the propellant acceleration.

erosion, massive electrical components, and low efficiencies (with their associated heat dissipation) have slowed implementation of these devices.

Hall-Effect Thrusters. When plasma densities are low enough and/or magnetic fields are high enough, the Hall-effect electric field becomes quite significant. This is the same phenomenon that is observed in the semiconductor Hall effect where a voltage arises transverse to the applied electric field. The Hall current can be understood to represent the motion of the electron "guiding center" (Ref. 19–7) in a crossed electric and magnetic field arrangement where collisions must be relatively insignificant. The Hall thruster is of interest because it represents a practical operating region for space propulsion, which Russian scientists were the first to successfully exploit in a design originally called the *stationary plasma thruster* or SPT, since a portion of the electron current "swirls in place" (Ref. 19–17).

In order to understand the principle of the Hall thruster it is necessary to rewrite in scalar form the generalized Ohm's law, Eq. 19-12. Because the electron Hall parameter $\beta = \omega \tau$ is no longer negligible, we arrive at two equations, which are (in Cartesian form):

$$j_x = \frac{\sigma}{1 + \beta^2} [E_x - \beta (E_y - v_x B_z)]$$
 (19–28)

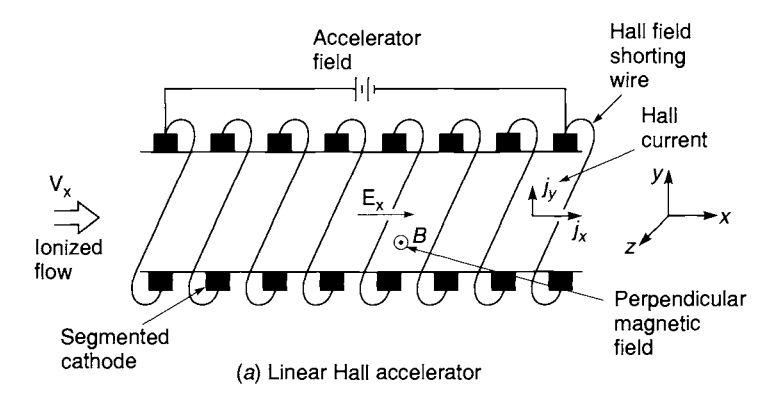
$$j_{y} = \frac{\sigma}{1 + \beta^{2}} [(E_{y} - v_{x}B_{z}) + \beta E_{x}]$$
 (19–29)

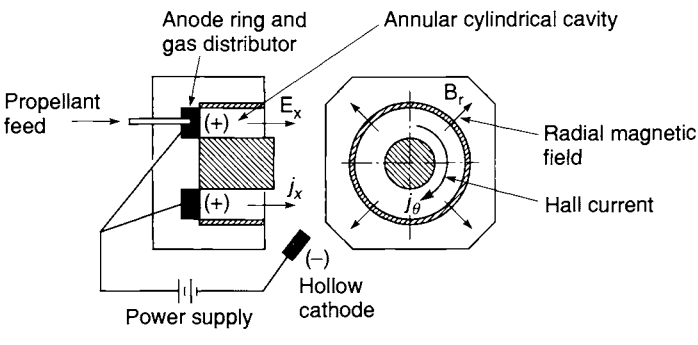
For a typical design, the application of a longitudinal electric field E_x causes a current density j_x to flow in the applied field direction together with a Hall current density j_y which flows in the direction transverse to E_x . The Hall electric field E_y is externally shorted to maximize that current and the electrodes are "segmented" in order not to short out the axial electric field E_x . Note that $\beta E_x > v_x B_z$. This arrangement results in a reasonably complicated design (see Fig. 19–10a), one which was deemed impractical. As will be discussed next, for space propulsion, engineers prefer the cylindrical geometry over the rectangular. It yields a simpler, more practical design; here the applied magnetic field is radial and the applied electric field is axial; the thrust-producing Hall current j_θ is azimuthal and counterclockwise and, because it closes on itself, it automatically shorts out its associated Hall electric field. The relevant geometry is shown in Fig. 19–10b, and the equations now become

$$j_x = \frac{\sigma}{1 + \beta^2} [E_x + \beta v_x B_r]$$
 (19–30)

$$j_{\theta} = \frac{\sigma}{1 + \beta^2} [\beta E_x - v_x B_r] \tag{19-31}$$

where, for an accelerator, $\beta E_x > v_x B_r$.



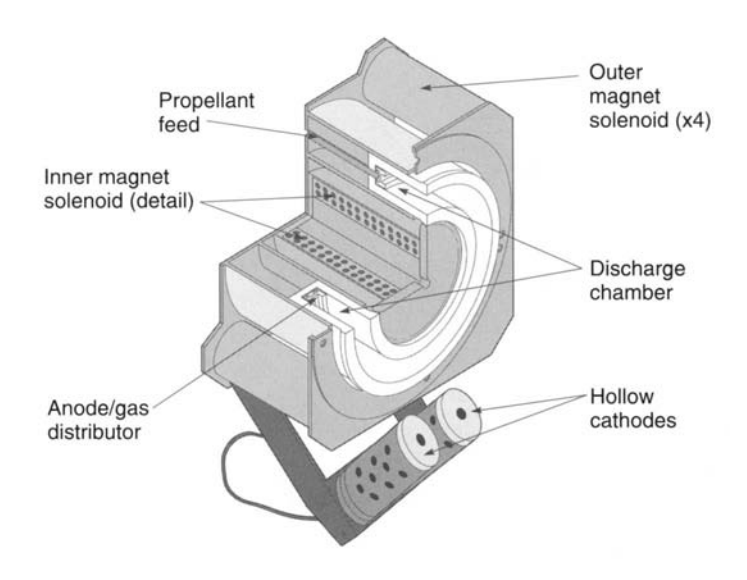


(b) Cylindrical Hall accelerator

FIGURE 19–10. Linear and cylindrical Hall accelerator configurations showing how an applied axial field results in a transverse current that accelerates the plasma. The Hall current peaks when the external resistance is absent (i.e., shorted). The presence of any significant axial current density j_x represents an inefficiency in Hall devices.

The current j_x is needed for ionization (by electron bombardment) because here the discharge chamber coincides with a portion of the accelerator region. The Hall current j_θ performs the acceleration through the Lorentz force $j_\theta B_r$. The Hall parameter is calculated from the product of the electron cyclotron frequency (Ref. 19–7) $\omega = eB/\mu_e$ and the collision time τ of the electrons with the heavier particles, which is part of the electrical conductivity in Eq. 9–11. In order for a Hall generator to be of interest, the electron Hall parameter must be much greater than one (in fact, Ref. 19–18 indicates that it should be at least 100), whereas ion motion must proceed relatively unaffected by magnetic effects. Large electron Hall parameters are obtained most readily with low plasma densities which translate into large times between collisions. Figure 19–11 shows a cutout of an SPT design with a redundant set of hollow cathodes and the solenoid magnetic pair responsible for the magnetic field. In Hall thrusters, the propellant gas, xenon or argon, is fed in the vicinity of the anode;

some gas is also provided through the cathode for more efficient cathode operation. While the discharge chamber is not physically separated from the accelerator region, the absence of ions in the first portion of the chamber effectively differentiates the ionization region from the rest of the accelerator. The local charge mass and density of the ions and electrons, together with the magnetic field profiles, need to be tailored such that the ion motion is mostly axial and the electron motion mostly spiral; this makes any given physical design inflexible to changes of propellant. A variation of the original nonconducting accelerator wall SPT design is a smaller channel with metallic walls;



NOMINAL CHARACTERISTICS

Propellant	Xenon
Thrust	83 milli N
Specific impulse	1600 sec
Efficiency (thruster)	0.48
Electric power	1350 watts
Mass flow rate	5.3 millgram/s
Design total impulse	1,000,000 N-sec
Design cycles	4000
Thruster mass	3.5 k g
Thruster dimensions	$15 \times 22 \times 12.5$ cr

FIGURE 19-11. External view and quarter section of a 1350-watt Hall accelerator (SPT). It is rated at a thrust of 83 mN and a specific impulse of 1600 sec. The radial magnetic field is produced by an inner solenoid and four external solenoids. Ionization takes place at the beginning of the insulated annular channel. The accompanying table lists the nominal characteristics of SPT-100. (Drawing courtesy of Atlantic Research Corporation and FAKEL.)

this "thruster with an anode layer" (TAL) has comparable performance with a higher thrust density.

The Hall thruster may be classified as either an electromagnetic device (as above) or an electrostatic device where the space charge in the ion acceleration region is neutralized by an electron current transverse to the ion flow (Refs. 19–17, 19–18). If we can mentally separate the process of ionization from that of acceleration, then it is easy to see that electrons swirling within the accelerator neutralize the ionic space charge as it moves from anode to cathode. This, in effect, decreases the magnitude of the accelerating fields and removes most of the beam-focusing requirements. In reality, there is some small interaction between the azimuthal electron current and the ion current, but it diminishes in proportion to the magnitude of the Hall parameter β .

The Hall thruster yields the best β -efficiency (η_H as defined below) when β is very large. The high β -limit is found, from Eqs. 19–30 and 19–31 and the definition of the plasma conductivity σ (Eq. 19–11), as

$$j_x \to \sigma v_x B_r / \beta = \rho_e v_x$$
 and $j_\theta \to \sigma E_x / \beta$ (19–32)

$$\tilde{F} = j_{\theta} B_r \to \rho_{\rho} E_x \tag{19-33}$$

$$\eta_H = \tilde{F}v_y/j_y E_y \to 1.0 \tag{19-34}$$

As can be seen, the accelerating force at this high Hall parameter limit is the electrostatic force and, since the exit ionization levels are about 90%, this corresponds in principle to the ion engine without any of its severe space-charge current limitations. Even though electron densities are in the order of 10^{15} to $10^{17}/\text{m}^3$, the effective space-charge densities (ρ_e) are considerably lower because of positive ion neutralization and approach zero at the exit. Furthermore, the Hall β -efficiency η_H as defined in the equations above reflects strictly the influence of β ; this efficiency is ideal, being an internal parameter that represents the loss that arises from the total current vector not being perfectly normal to the flow direction. The overall efficiency is still given by Eq. 19–2.

Example 19-3. (a) For the SPT-100 information given in Fig. 19-11, verify the values of thrust and efficiency. (b) Using the definition of the Hall efficiency above, calculate its value for $\beta = 200$ and for a representative value of the parameter $B_r v_x / E_x = 2.5 \times 10^{-2}$ (this grouping of variables can be shown to be intrinsic in the Hall thruster).

SOLUTION. (a) The mass flow rate is 5.3×10^{-6} kg/sec, the specific impulse is 1600 sec, and the input power is 1350 W. Hence

$$F = \dot{m} I_s g_0 = (5.3 \times 10^{-6})(1600)(9.81) = 83.2 \text{ mN}$$

 $\eta_t = F I_s g_0 / 2P_e = (8.3 \times 10^{-2})(1600)(9.81) / 2(1350) = 48.4\%$

Both of these answers compare very well with the information in Fig. 19–11.

(b) With some manipulation, and defining the Hall local efficiency parameter $\xi = B_r v_x / E_x$, Eq. 19-34 can be written as

$$\eta_H = (-\xi + \beta)\xi/(1 + \beta\xi) = 5/6 = 83.3\%$$

Since the parameter ξ can be highly variable across real accelerator channels, this Hall β -efficiency is not necessarily representative of the overall efficiency, only of the maximum efficiency. Clearly, even the ideal Hall accelerator is not as good as the ideal Faraday or MPD accelerator. Nevertheless, for very large values of β , it can be seen that this efficiency will approach one for any value of ξ .

19.4. OPTIMUM FLIGHT PERFORMANCE

Now that we have discussed the various propulsion devices available, we return to the discussion of flight performance. In Section 19.1 the fundamental background for an optimum propulsion system design was introduced. The discussion remained incomplete because the specific power and the efficiency of individual thrusters, among other things, need to be known for further analysis. In a given mission, the payload m_{pl} and velocity increment Δu are specified along with upper limits on electric power available (Ref. 19-19). In the analysis of Section 19.1, for any desired $\Delta u/v_c$, one can find an optimum v/v_c given a payload ratio; however, even when the choice of an electric propulsion system has been made, thrust time t_p is unspecified and thus the total mass also remains unspecified. Thrust time or "burn time" is the smallest for zero payload and continuously increases with increasing payload ratio. Concurrently, the specific impulse changes, making the problem underconstrained.

Given the payload mass and the vehicle velocity increment, a spacecraft design procedure might be followed using the optimum results of Section 19.1, e.g.:

- 1. Pick a payload mass fraction—from Fig. 19–3 this yields an optimum $\Delta u/v_c$.
- 2. From the given Δu , deduce the value of the characteristic speed v_c .
- 3. From the optimum value of v/v_c in Fig. 19-3 at the given mass fraction, or Eq. 19-9, calculate the corresponding value of v or I_s .
- 4. Select an engine that can deliver this optimum I_s and from its characteristics (i.e., α and η_t) find the thrusting time t_p from Eq. 19-8.
- 5. Calculate m_p from Section 19.1, including Eq. 4–7 and the given payload ratio.
- Check that the available vehicle electrical power (from Eq. 19-6) together
 with vehicle volume plus the desirable mission time and total cost are not
 exceeded.

As may be evident, a unique criterion for the choice of the assumed payload mass fraction is missing above. One possible solution to this problem is to look for a "dual optimum", namely, to seek the shortest burn time consistent with the highest payload mass fraction. A maximum for the product of m_{pl}/m_0 with $\Delta u/v_c$ does exist as a function of v/v_c (as shown in Ref. 19–20). In other words, this dual optimum defines a minimum overall mass for a specified payload consistent with minimum transfer time. Table 19–7 gives estimated values of α along with the corresponding range of specific impulse and the efficiency for electric propulsion systems in present engine inventories.

The optimum formulation in Section 19.1, however, needs to be modified to account for the portion of tankage mass which results from propellant loading; with few exceptions, an additional 10% of the propellant mass shows up as tank or container mass (this could be further refined to include reserve propellant). Reference 19–16 includes information on this tankage fraction for various thrusters. Fortunately, the analysis presented earlier is little modified and it turns out that the optima are driven toward higher specific impulses and longer times of operation. For an arbitrary tankage fraction allowance φ ,

$$\frac{\Delta u}{v_c} = \frac{v}{v_c} \ln \left[\frac{(1+\varphi) + (v/v_c)^2}{(m_{pl}/m_0 + \varphi) + (v/v_c)^2} \right]$$
(19–35)

When $\varphi=0.1$ the actual value for the joint-optimized payload ratio can be shown to be 0.46, with corresponding ratios of vehicle velocity increment as 0.299 and propellant exhaust velocity as 0.892. It turns out that this peak is rather broad and that payload ratios between 0.34 and 0.58 are within 6% of the mathematical optimum. Since engine parameters are rather "inelastic", and since spacecraft designers have to deal with numerous constraints which are not propulsion related, this wider range of optima is deemed a practical necessity.

Given the desirable 0.34 to 0.58 optimum payload-ratio range, we may first select one or more engines within the range $0.2268 \le (I_s^*/\Delta u) \le 0.4263$, where the optimized specific impulse (I_s^*) is in sec and the velocity change in m/sec. Since the vehicle's change in velocity is known, this condition yields the required limits in specific impulse. We can then proceed to use the following joint-optimized, approximate polynomial relations to find m_{pl}/m_0 and t_p^* as follows:

TABLE 19-7. Summary of Current Technology in Typical Electric Propulsion Engines

Engine Type	Identification (Reference)	Specific power, α (W/kg) (estimated)	Thruster Efficiency, η_t	Specific Impulse, I_s (sec)	Power (W)	Thrust (N)	Lifetime (hr)	Status
Resistojet	N ₂ H ₄ (16, 21) (19–16, 19–21) NH ₃ (19–16) Primex MR-501B (19–21)	333~500	0.8-0.9	280-310 350 303-294	500-1500 500 350-510	0.2-0.8 0.369-0.182	> 390	Operational
Arcjet	N ₂ H ₄ (19–21) H ₂ (19–16, 19–21)	313 333	0.33-0.35 0.4	450–600 1000	300-2000 5-100 K	0.2-0.25 0.2-0.25	> 830-1000 > 1000	Operational Operational R&D
	NH ₃ (19–16) Primex Mr-509 (19–21) (c) Primex MR-510 (19–21) (c)	270–320 115.3 150	0.27-0.36 > 0.31 > 0.31	500-800 > 502 (545) > 570-600	50030 K 1800 2170	0.2-0.25 0.213-0.254 0.222-0.258	1500 > 1575 > 2595	Qualified Qualified Qualified
Ion Propulsion	XIPS (19–21) Hughes XIPS-13 (19–21) Hughes XIPS-25 (19–21) NSTAR/DS1 (19–13) RITA 15 (a) UK-10/T5 (UK) (19–21) ETS-VI IES (Jap.) (19–21) DASA RIT-10 (Ger.) (19–21)	100 45 9.61	0.75 0.46, 0.54 0.65, 0.67 0.6 0.55-0.64 0.4 0.38	2800-3500 2585, 2720 2800 3100 3000 4000 3090-3300 3000-3150	200-4000 427, 439 1400 2300-2500 540 278-636 730 585	0.015-0.014 0.0178, 0.018 0.0635 0.093 0.015 0.010-0.025 0.02 0.015	> 8000 12,000 > 4350 > 10,000 > 20,000 10,700	Operational Qualified Qualified Operational Qualified Qualified Operational Operational
Hall	Hall (XE) (19-16) SPT (XE) (19-21) ARC/Fakel SPT-100 (19-16) Fakel SPT-70 (19-3) TAL D-55 (Russia) (19-21) Primex BPT Hall (c)	150 169.8 ~ 50.9	0.5 0.48 0.48 0.46, 0.50 0.48, 0.50–0.60 0.5	1500 -1600 1600 1600 1510, 1600 950-1950 1500-1800	3006000 1501500 1350 640660 6001500 5006000	0.04 0.04 0.2 0.083 0.04 0.082	> 7000 > 4000 > 7424 9000 > 5000	Operational Operational Operational Operational Development
MPDSteady	Applied Field (19-16) Self-field (19-16)		0.5 0.3	2000-5000 2000-5000	1-100 K 200-4000 K			R&D R&D
MPD-Pulsed	Teflon PPT (19–16) LES 8/9 PPT (19–21) NASA/Primex EO-1 (c) Primex PRS-101 (c) EPEX arcjet (Jap.) (19–21)	1 ~ 20	0.07 0.0068, 0.009 0.098 0.16	1000 836, 1000 1150 1150 600	1–200 25, 30 up to 100 430	4000 N-sec 0.0003 3000 N-sec 1.4 mN, 2 Hz 0.023	> 10 ⁷ pulses > 10 ⁷ pulses	Operational Operational Operational Operational Operational

Manufacturers: (a): Daimler-Chrysler Aerospace, AG., (b): Atlantic Research Corporation, USA Fakel (Russia), (c): Primex Aerospace Company

$$\frac{m_{pl}}{m_0} \approx \left[-0.1947 + 2.972 \left(\frac{I_s^*}{\Delta u} \right) - 2.7093 \left(\frac{I_s^*}{\Delta u} \right)^2 \right]$$
 (19–36)

$$t_p^* \approx \left[67.72 - 39.67 \left(\frac{m_{pl}}{m_0} \right) + 20.04 \left(\frac{m_{pl}}{m_0} \right)^2 \right] \frac{(I_s^*)^2}{\alpha \eta_t} (\text{sec})$$
 (19–37)

The success of this approach hinges on the validity of the engine information employed. In particular, the specific power should represent all the inert components of the engine, which can be reasonably assumed to depend on the power level. The payload mass must reflect all mass that is neither proportional to the electrical power nor propellant related. The tankage fraction allowance must reflect the total propellant mass and thus the use of Eq. 19–35 is necessary. It is assumed that there is available a source of electricity (typically from 28 to 110 V DC for solar-powered craft) which is not tagged to the propulsion system. The analysis also assumes that the efficiency is not a function of specific impulse (in contrast to Ref. 19–22); this implies that an average or effective value can be used. Since each individual engine type spans a somewhat limited range of specific impulse, this assumption is not deemed to be too restrictive. For the continuous thrust schedules required by electric engines, thrust time is equal to mission time.

Example 19–4. List the performance of three electric propulsion engines within the dual-optimum criteria to carry a 100 kg payload through a change of velocity of 7000 m/sec. Calculate total mass, burn time, thrust, and power requirements.

SOLUTION. We first calculate the dual-optimum specific-impulse range, which turns out to be between 1590 sec and 2980 sec. Then, we pick engines from the inventory (see Table 19–7). Results are tabulated below for three thrusters.

$$0.2268\Delta u \le I_s^*[\sec] \le 0.4263\Delta u$$

$$m_0 = 100/(m_{pl}/m_0) = 100 + 1.1m_p + m_{pp} = 100 + m_p(1.1 + (v/v_c)^2)$$

$$(v/v_c)^* = 0.6953 + 0.5139(m_{pl}/m_0) - 0.1736(m_{pl}/m_0)^2$$

Hall Effect Thruster	Xenon Ion Propulsion System	Magnetoplasma Dynamic
$I_s^* = 1600 \text{ sec}$	$I_s^* = 2585 \text{ sec}$	$I_s^* = 3000 \text{ sec}$
$\alpha \eta_t = 93.5 \text{ W/kg}$	$\alpha \eta_t = 46 \text{ W/kg}$	$\alpha \eta_t = 30 \text{ W/kg}$
(Demonstrated)	(Demonstrated)	(Experimental)
$m_{pl}/m_0 = 0.343, m_0 = 291 \text{ kg}$	$m_{pl}/m_0 = 0.533, m_0 = 187 \text{ kg}$	$m_{pl}/m_0 = 0.581, m_0 = 172 \text{ kg}$
$t_p^* = 17.9 \text{ days}$	$I_p^* = 87.9 \text{ days}$	$t_p^* = 178 \text{ days}$
F = 1.06 N	F = 0.149 N	F = 69.7 mN
$P_e = 15.4 \text{ kW}$	$P_e = 4.12 \text{ kW}$	$P_e = 2.05 \text{ kW}$

As can be seen, total mass, along with thrust, decreases with increasing specific impulse, whereas thrust time increases. The power variation P_e also decreases, reflecting the individual choice of engines and the engine data from Table 19–7. Any engine can be

eliminated when the required power exceeds the power available in the spacecraft or when the burn time exceeds some specified mission time constraint. Most often, cost is the ultimate selection criterion and is largely dependent on m_0 .

19.5. MISSION APPLICATIONS

Three principal application areas have been described in the introduction to this chapter. The selection of a particular electric propulsion system for a given flight application depends not only on the characteristics of the propulsion system (which are described in this chapter) but also on the propulsive requirements of the particular flight mission, the proven performance of the specific candidate propulsion system, along with vehicle interfaces and the power conversion and storage systems. In general, the following criteria can be enumerated:

- 1. For very precise low-thrust station-keeping and attitude control applications, *pulsed thrusters* are generally best suited.
- 2. For deep space missions where the vehicle velocity increment is appreciably high, systems with *very high specific impulse* will give better performance. As shown in Section 19.1, the optimum specific impulse is proportional to the square root of the thrust operating time.
- 3. The higher the specific impulse, the more electrical power is required for a given thrust level. This translates into larger size and mass requirements for the power conditioning and generating equipment. However, for a given payload and vehicle velocity increase, the total mass and the thrust vary in nontrivial ways with respect to the specific impulse (see Example 19–4).
- 4. Since most missions of interest require long life, system reliability is a key selection criterion. Extensive testing under all likely environmental conditions (temperatures, pressures, accelerations, vibration, and radiation conditions) is required for high reliability. Ground testing and qualification of electric engines should be no different from that of their chemical counterparts, where large resources have made it possible to develop the present inventory of reliable engines. Simulation of the low pressures in space requires large vacuum test chambers.
- 5. There is a premium on high thruster efficiency and high power-conversion efficiency. This will reduce the inert mass of the power supply system and reduce thermal control requirements, all of which usually results in lower total mass and higher vehicle performance.
- 6. For every propulsion mission there is a theoretically *optimum range of specific impulse* (see Fig. 19–3) and thus an optimum electrical propulsion system design. While this optimum may be blurred by some conflicting system constraints (e.g., flight time or maximum power or size con-

straints or cost), the present variety in the engine inventory can meet most goals.

- 7. The present *state of the art in electrical power sources* appears to limit the type and size of electric propulsion systems that can be integrated, particularly for missions to the outer planets, unless nuclear energy power generation on board the spacecraft becomes more developed and acceptable.
- 8. Practical factors, such as the storing and feeding of liquids in zero gravity, the availability of propellant (in the case of xenon), the conditioning of power to the desired voltage, frequency, and pulse duration, as well as the redundancy in key system elements, the survival of sensors or controllers in long flights, and the inclusion of automatic self-checking devices along with cost, will all influence the selection and application of specific types of electric rockets.
- 9. In addition to tankage considerations, *propellant selection* will also be influenced by certain interface criteria such as plume noninterference with communication signals. Plumes must also be thermally benign and noncondensing on sensitive surfaces of the spacecraft such as optical windows, mirrors, and solar cells.

Synchronous or geostationary satellites are extremely attractive for communications and earth observation; their long life requires extensive station-keeping propulsion requirements. Until recently, the main limitation to any such life increase had been the propellant requirement. There is also a propulsion need for orbit raising from LEO to GEO. Earth satellites in inclined orbits with precise time–trajectory position requirements need propulsion units to maintain such orbits, counteracting certain perturbing natural forces described in Chapter 4.

The increasing life trend in earth-orbit satellites from a minimum of 8 years to at least 15 years significantly increases their total impulse and durability requirements of the propulsion system. For example, the north-south station-keeping (NSSK) function of a typical geosynchronous satellite requires about 40,000 to 45,000 N-sec or 9000 to 10,000 lbf-sec of impulse per year. Table 19–8 shows some of the characteristics required of small and large electric thrusters for various propulsion functions in space.

19.6. ELECTRIC SPACE-POWER SUPPLIES AND POWER-CONDITIONING SYSTEMS

The availability of substantial amounts of electrical power in space is considered to be one of the most significant factors in electrical propulsion. Several combinations of energy sources and conversion methods have reached prototype stages, but only solar cells (photovoltaic), isotope thermoelectric genera-

TABLE 19–8.	Space Propulsion	Application and	Characteristics	for Three	Thrust
Levels of Elec	tric Propulsion Thr	rusters			

Thrust Class	Application (Life)	Characteristics	Status
Micronewtons (μN)	E-W station keeping Attitude control Momentum wheel unloading (15-20 years)	10–500 W power Precise impulse bits of $\sim 2 \times 10^{-5}$ N-sec	Operational
Millinewtons (mN)	N-S station keeping Orbit changes Drag cancellation Vector positioning (20 years)	Kilowatts of power Impulse bits $\sim 2 \times 10^{-3}$ N-sec for N-S, impulse/year of 46,000 N-sec/100 kg	Operational
0.2 to 10 N	Orbit raising Interplanetary travel Solar system exploration (1-3 years)	spacecraft mass Long duration 10–300 kW of power Intermittent and continuous operation	In development

tion units (nuclear), and fuel cells (chemical) have advanced to the point of routine space-flight operation. Power output capacity of operational systems has been increasing from the low one-kilowatt range to the medium tens of kilowatts required for some missions. The high end of a hundred or more kilowatts is still pending some technological (and political) breakthroughs.

Space power level requirements have been increasing with the increased capacity of earth-orbit communications satellites and with planned missions, manned and robotic, to the moon and nearby planets. Payload requirements and thrust duration dictate the power level. Commercial communications satellites can temporarily reduce the communications volume during orbit maintenance so that the electric power does not require a dedicated power supply for the propulsion system, but larger power demands require enhanced solar cell capabilities. Some communications satellites actually share part or all of the power-conditioning equipment with their electric thrusters.

Power Generation Units

Electric power-generation units are classified as either direct (no moving mechanical parts) or dynamic. When the primary driver is reliability and the total power is small, direct conversion has been preferred but, with the advent of the Space Shuttle and with the proposed manned space station, dynamic systems are being reconsidered. Many diverse concepts have been evaluated for meeting the electrical power demands of spacecraft, including electric propul-

sion needs. Direct energy conversion methods considered include photovoltaic, thermoelectric, thermionic, and electrochemical, while indirect methods (with moving parts) include the Brayton, Rankine, and Stirling cycles.

Batteries. Batteries can basically be classified as either primary or secondary. *Primary batteries* consume their active materials and convert chemical energy into electrical. *Secondary batteries* store electricity by utilizing a reversible chemical reaction and are designed to be recharged many times. There are both dry-cell and wet-cell primary batteries. The importance of primary batteries passed with the short-lived satellites of the early 1960s. Secondary batteries with recharging provisions provide electrical power at output levels and lifetimes longer than primary batteries. Batteries must be sealed against the space vacuum or housed inside pressurized compartments. Secondary batteries are a critical component of solar cell systems for power augmentation and emergency backup and the periods when the satellite is in the earth's shadow.

Fuel Cells. Chemical fuel cells are conversion devices used to supply space-power needs for 2 to 4 weeks and for power levels up to 40 kW in manned missions. A catalyzer controls the reaction to yield electricity directly from the chemical reaction; there is also some heat evolved, which must be removed to maintain a desirable fuel cell temperature. They are too massive for both robotic and long-duration missions, having also had some reliability problems. Recent improvements in fuel cell technology have considerably advanced their performance.

Solar Cell Arrays. Solar cells rely on the photovoltaic effect to convert electromagnetic radiation. They have supplied electrical power for most of the long-duration space missions. The first solar cell was launched in March 1958 on Vanguard I and successfully energized data transmission for 6 years. Solar arrays exist in sizes up to 10 kW and could potentially grow to 100 kW sizes in earth orbits.

An *individual cell* is essentially one-half of a p-n junction in a transistor, except that the surface area has been suitably enlarged. When exposed to sunlight, the p-n junction converts photon energy to electrical energy. Typically, solar cell arrays are designed for 20% over-capacity to allow for material degradation toward the end of life. Loss in performance is due to radiation and particle impact damage, particularly in the radiation belts around the earth. There has been some improvement in efficiency, reliability, and power per unit mass. For example, standard silicon cells deliver 180 W/m² and arrays have 40 W/kg. Newer gallium arsenide cells produce 220 W/m² and are more radiation resistant than silicon cells; gallium arsenide cells are presently space qualified and integrated; together with parabolic concentrators, their arrays can reach 100 W/kg (Ref. 19-16). In the near future, multi-junction solar

cells designed to utilize a greater portion of the solar spectrum will be used; they have already demonstrated 24% efficiency.

Factors that affect the specific mass of a solar array, besides conversion efficiency, include the solar constant (which varies inversely as the square of the distance from the sun) and the manufactured thinness of the cell. Orientation to the sun is a more critical factor when solar concentrators are being used. Cell output is a function of cell temperature; performance can suffer as much as 20% for a 100°F increase in operating temperature so that thermal control is critical. Solar cell panels can be (1) fixed and body mounted to the spacecraft, (2) rigid and deployable (protected during launch and positioned in space), (3) flexible panels that are deployed (rolled out or unfolded), and (4) deployed with concentrator assist.

In addition to the solar arrays, their structure, deployment and orientation equipment, other items including batteries, plus power conditioning and distribution systems are assigned to the power source. Despite their apparent bulkiness and battery dependence, solar-cell electrical systems have emerged as the dominant generating power system for unmanned spacecraft.

Nuclear Thermoelectric and Thermionic Systems. Nuclear energy from long-decay radioisotopes and from fission reactors has played a role in the production of electricity in space. Both thermoelectric (based on the Seebeck effect) and thermionic (based on the Edison effect) devices have been investigated. These generators have no moving parts and can be made of materials reasonably resistant to the radioactive environment. But their specific power is relatively low and cost, availability, and efficiency have been marginal.

Throughout the 1950s and 1960s nuclear fission reactors were regarded as the most promising way to meet the high power demands of space missions, particularly trips to the outer planets involving months and perhaps years of travel. Radioisotope thermoelectric power has been embodied in a series of SNAP (Systems for Nuclear Auxiliary Power) electrical generating units which were designed and tested, ranging from 50 W to 300 kW of electrical output. Fission reactors were included in the SPAR (Space Power Advance Reactor) program, later renamed SP-100, which was to feature a nuclear-thermoelectric generator with an electrical output of 100 kW; this program was discontinued in 1994. The most recent space nuclear reactor generator is the Russian TOPAZ that has been space tested up to nearly 6 kW. It consists of sets of nuclear rods each surrounded by a thermionic generator. TOPAZ technology was obtained by the USA from the Russians and efforts to upgrade and flight-qualify the system were underway in the mid-1990s.

Thermionic converters have a significant mass advantage over thermoelectric ones, based on their higher effective radiator temperatures. Since thermal efficiencies for both thermoelectric and thermionic conversion are below 10% and since all unconverted heat must be radiated, at higher temperatures thermionic radiators are less massive. Moreover, cooling must be present at times

when no electricity is generated since the heat source cannot be "turned off." Depending on the location of the waste heat, clever designs are needed, involving heat pipes or recirculating cooling fluids.

Long-Duration High-Output Dynamic Systems. Designs of electric power generation with outputs of 10 to 1000 kW here on earth have been based on Stirling or Rankine heat engine cycles with nuclear, chemical, and even solar power sources. Overall efficiencies can be between 10 and 40%, but the hardware is complex, including bearings, pumps, reactors, control rods, shielding, compressors, turbines, valves, and heat exchangers. Superconducting magnets together with advances in the state-of-the-art of seals, bearings, and flywheel energy storage have made some dynamic units relatively more attractive. There remain development issues about hightemperature materials that will withstand intense nuclear radiation fluxes over several years; there are still some concerns about achieving the required reliability in such complex systems in the space environment. While limited small-scale experiments have been conducted, the development of these systems remains a challenge. The potential of flight accidents, i.e., the unwanted spreading of nuclear materials, remains a concern for the launch and in manned space missions.

Power-Conditioning Equipment

Power-conditioning equipment is a necessary part of electric propulsion systems because of inevitable mismatches in voltage, frequency, power rate, and other electrical properties between the space-power generating unit and the electric thruster. In some earlier systems, the power-conditioning equipment has been more expensive, more massive, and more difficult to qualify than the thruster itself. If the thrust is pulsed, as in the PPT, the power-conditioning unit has to provide pulse-forming networks for momentary high currents, exact timing of different outputs, control and recharging of condensers. Ion engines typically require from 1000 to 3000 V DC; the output of solar-cell arrays is 28 to 300 V DC so there is a need for DC-to-DC inverters and step-up transformers to accomplish the task. Often this equipment is housed in a single "black box," termed the power conditioner. Modern conditioning equipment contains all the internal logic required to start, safely operate, and stop the thruster; it is controlled by on-off commands sent by the spacecraft-control processor. Besides the above functions that are specific to each engine, power-conditioning equipment may provide circuit protection and propellant flow control as well as necessary redundancies.

As may be apparent from Table 19–7, one of the largest contributors to the specific mass of the system (α) is the power-conditioning equipment. Here, electrothermal units have the simplest and lightest conditioning equipment. Ion engines, on the other hand, have the heaviest equipment, with Hall thrusters somewhere in between (Ref. 19–17). PPTs tend to be heavy, but advances

in energy storage capacitors can improve this situation. In fact, advances in solid-state electronic pulse circuits together with lighter, more efficient, and higher temperature power-conditioning hardware are an area of great interest to the implementation of electric propulsion units. The efficiency of the equipment tends to be high, about 90% or more, but the heat generated is at a low temperature and must be removed to maintain the required moderately low temperatures of operation. When feasible, the elimination of conditioning equipment is desirable, the so-called direct drive, but a low-pass filter would still be necessary for electromagnetic interference (EMI) control (more information in Ref. 19–21).

PROBLEMS

- 1. The characteristic velocity $v_c = \sqrt{2t_p\alpha\eta}$ was used to achieve a dimensionless representation of flight performance analysis. Derive Eq. 19–35 without any tankage fraction allowance. Also, plot the payload fraction against v/v_c for several values of $\Delta u/v_c$. Discuss your results with respect to optimum performance.
- 2. For the special case of zero payload, determine the maximized values of $\Delta u/v_c$, v/v_c , m_p/m_0 , and m_{pp}/m_0 in terms of this characteristic velocity as defined in Problem 1. Answer: $\Delta u/v_c = 0.805$, $v/v_c = 0.505$, $m_p/m_0 = 0.796$, $m_{pp}/m_0 = 0.204$.
- 3. For a space mission with an incremental vehicle velocity of 85,000 ft/sec and a specific power of $\alpha = 100$ W/kg, determine the optimum values of I_s and t_p for two maximum payload fractions, namely 0.35 and 0.55. Take the thruster efficiency as 100% and $\varphi = 0$.

Answer: for 0.35: $I_s = 5.11 \times 10^3$ sec; $t_p = 2.06 \times 10^7$ sec; for 0.55: $I_s = 8.88 \times 10^3$ sec; $t_p = 5.08 \times 10^7$ sec.

- **4.** Derive Eq. 19–7 showing v_c explicitly.
- 5. An electric rocket uses heavy charged particles with a charge-to-mass ratio of 500 coulombs per kilogram producing a specific impulse of 3000 sec. (a) What acceleration voltage would be required for this specific impulse? (b) If the accelerator spacing is 6 mm, what would be the diameter of an ion beam producing 0.5 N of thrust at this accelerator voltage?

 Answers: (a) 8.66 × 10⁵ V; (b) D = 1.97 mm.
- Answers. (a) 6.00×10^{-4} V, (b) D = 1.97 Hilli.
- 6. An argon ion engine has the following characteristics and operating conditions: Voltage across ionizer = 400 V Voltage across accelerator = $3 \times 10^4 \text{ V}$ Diameter of ion source = 5 cm Accelerator electrode spacing = 1.2 cm Calculate the mass flow rate of the propellant, the thrust, and the thruster overall efficiency (including ionizer and accelerator). Assume singly charged ions.

 Answer: $\dot{m} = 2.56 \times 10^{-7} \text{ kg/sec}$; $F = 9.65 \times 10^{-2} \text{ N}$; $\eta_t = 98.7\%$
- 7. For a given power source of 300 kW electrical output, a propellant mass of 6000 lbm, $\alpha = 450$ W/kg, and a payload of 4000 lbm, determine the thrust, ideal velocity increment, and duration of powered flight for the following three cases:
 - (a) Arcjet $I_s = 500 \text{ sec}$ $\eta_t = 0.35$

- (b) Ion engine $I_s = 3000 \text{ sec}$ $\eta_t = 0.75$ (c) Hall engine $I_s = 1500 \text{ sec}$ $\eta_t = 0.50$ Answers:
- (a) $t_p = 3.12 \times 10^5 \text{ sec}$; $\Delta u = 3.63 \times 10^3 \text{ m/sec}$; F = 42.8 N(b) $t_p = 5.24 \times 10^6 \text{ sec}$; $\Delta u = 2.18 \times 10^4 \text{ m/sec}$; F = 15.29 N(c) $t_p = 1.69 \times 10^6 \text{ sec}$; $\Delta u = 1.09 \times 10^4 \text{ m/sec}$; F = 20.4 N
- 8. A formulation for the exit velocity that allows for a simple estimate of the accelerator length is shown below; these equations relate the accelerator distance to the velocity implicitly through the acceleration time t. Considering a flow at a constant plasma of density ρ_m (which does not choke), solve Newton's second law first for the speed v(t) and then for the distance x(t) and show that

$$v(t) = (E_y/B_z)[1 - e^{-t/\tau}] + v(0)e^{-t/\tau}$$

$$x(t) = (E_y/B_z)[t + \tau e^{-t/\tau} - \tau] + x(0)$$

where $\tau = \rho_m/\sigma B_z^2$ and has units of sec. For this simplified plasma model of an MPD accelerator, calculate the distance needed to accelerate the plasma from rest up to v=0.01(E/B) and the time involved. Take $\sigma=100$ mho/m, $B_z=10^{-3}$ tesla (Wb/m²), $\rho_m=10^{-3}$ kg/m³, and $E_y=1000$ V/m. Answer: 503 m, 0.1005 sec

- 9. Assume that a materials breakthrough makes it possible to increase the operating temperature in the plenum chamber of an electrothermal engine from 3000 K to 4000 K. Nitrogen gas is the propellant which is available from tanks at 250 K. Neglecting dissociation, and taking $\alpha = 200 \text{ W/kg}$ and $\dot{m} = 3 \times 10^{-4} \text{ kg/sec}$, calculate the old and new Δu corresponding to the two temperatures. Operating or thrust time is 10 days, payload mass is 1000 kg, and k = 1.3 for the hot diatomic molecule. Answer: 697 m/sec old, 815 new.
- 10. An arcjet delivers 0.26 N of thrust. Calculate the vehicle velocity increase under gravitationless, dragless flight for a 28-day thrust duration with a payload mass of 100 kg. Take thruster efficiency as 50%, specific impulse as 2600 sec, and specific power as 200 W/kg. This is not an optimum payload fraction; estimate an I_s which would maximize the payload fraction with all other factors remaining the same. Answer: $\Delta u = 4.34 \times 10^3$ m/sec; $I_s = 2020$ sec (decrease).

SYMBOLS

acceleration, m/sec² (ft/sec²) area, cm² or m² a Amagnetic flux density, Web/m² or tesla В specific heat, J/kg-K c_p d accelerator grid spacing, cm (in.) hole or beam diameter, cm (in.) Delectronic charge, 1.602×10^{-19} coulomb e Eelectric field, V/m

```
f
          microscopic force on a particle
F
          thrust force, N or mN (lbf or mlbf)
\tilde{F}_{r}
          accelerating force density inside channel, N/m<sup>3</sup> (lbf/ft<sup>3</sup>)
          constant converting propellant ejection velocity units to sec, 9.81
g_0
          m/sec<sup>2</sup> or 32.2 ft/sec<sup>2</sup>
          total current, A
Ι
          specific impulse, sec [I_s^*] optimum]
I_{\circ}
i
          current density, A/m<sup>2</sup>
          orthogonal current density components
j_x, j_y
          Hall current density, A/m<sup>2</sup>
İθ
k
          specific heat ratio
l_I
          ionization loss, W
          propellant mass, kg (lbm)
m_{p}
m_{pp}
          power plant mass, kg (lbm)
m_{pl}
          payload mass, kg (lbm)
          initial total vehicle mass, kg (lbm)
m_0
          mass flow rate, kg/sec (lbm/sec)
m
\mathfrak{M}
          atomic or molecular mass, kg/kg-mol (lbm/lb-mol)
          electron number density, m^{-3} (ft<sup>-3</sup>)
n_e
p
          power, W
P_{\rho}
          electrical power, W
P_{iet}
          kinetic power of jet, W
R
          plasma resistance, ohms
S
          distance, cm (in.)
t
          time, sec
T^{p}
          propulsive time, sec [t_p^*] optimum]
          absolute temperature, K (R)
          vehicle velocity change, m/sec (ft/sec)
 \Delta u
v
          propellant ejection velocity, m/sec (ft/sec)
          plasma velocity along accelerator, m/sec
v_x
          characteristic speed
v_c
 V
          voltage, V
 V_{acc}
          accelerator voltage, V
          linear dimension, m (ft)
 x
```

Greek Letters

```
specific power, W/kg (W/lbm)
α
β
          electron Hall parameter (dimensionless)
          permittivity of free space, 8.85 \times 10^{-12} farad/m
\varepsilon_0
          ionization energy, eV
\varepsilon_I
           Hall thruster \beta-efficiency
\eta_H
          thruster efficiency
\eta_t
           ion mass, kg
\mu
          electron mass, 9.11 \times 10^{-31} \text{ kg}
\mu_{\rho}
```

- v_e charge particle velocity, m/sec
- ξ Hall thruster local efficiency parameter
- ρ_e space charge, coulomb/m³
- σ plasma electrical conductivity, mho/m
- τ mean collision time, sec (also characteristic time, sec)
- φ propellant mass tankage allowance
- ω electron cyclotron frequency, (sec)⁻¹

REFERENCES

- 19-1. R. G. Jahn, *Physics of Electric Propulsion*, McGraw-Hill Book Company, New York, 1968, pp. 103-110.
- 19–2. E. Stuhlinger, Ion Propulsion for Space Flight, McGraw-Hill Book Company, New York, 1964.
- 19-3. P. J. Turchi, "Electric Rocket Propulsion Systems," Chapter 9 in R. W. Humble, G. N. Henry, and W. J. Larson (Eds.), *Space Propulsion Analysis and Design*, McGraw-Hill, New York, 1995, pp. 509-598.
- 19–4. A. Spitzer, "Near Optimal Transfer Orbit Trajectory Using Electric Propulsion," AAS Paper 95-215, American Astronautical Society Meeting, Albuquerque, NM, 13–16 February 1995.
- 19–5. D. B. Langmuir, "Low-Thrust Flight: Constant Exhaust Velocity in Field-Free Space," in H. Seifert (Ed.), *Space Technology*, John Wiley & Sons, New York, 1959, Chapter 9.
- 19-6. C. D. Brown, Spacecraft Propulsion, AIAA Education Series, Washington, DC, 1996.
- 19-7. F. F. Chen, Introduction to Plasma Physics, Plenum Press, New York, 1974.
- 19-8. G. W. Sutton and A. Sherman, Engineering Magnetohydrodynamics, McGraw-Hill Book Company, New York, 1965.
- 19–9. D. M. Zube, P. G. Lichon, D. Cohen, D. A. Lichtin, J. A. Bailey, and N. V. Chilelli, "Initial On-Orbit Performance of Hydrazine Arcjets on A2100 Satellites," AIAA Paper 99-2272, June 1999.
- 19-10. T. Randolph, "Overview of Major U.S. Industrial Programs in Electric Propulsion," AIAA Paper 99-2160, June 1999.
- 19-11. R. L. Sackeim and D. C. Byers, "Status and Issues Related to In-Space Propulsion Systems," *Journal of Propulsion and Power*, Vol. 14, No. 5, September-October 1998.
- 19-12. J. R. Beattie, "XIPS Keeps Satellites on Track," *The Industrial Physicist*, Vol. 4, No. 2, June 1998.
- 19–13. J. Wang, D. Brinza, R. Goldstein, J. Polk, M. Henry, D. T. Young, J. J. Hanley, J. Nodholt, D. Lawrence, and M. Shappirio, "Deep Space One Investigations of Ion Propulsion Plasma Interactions: Overview and Initial Results," *AIAA Paper 99-2971*, June 1999.
- 19-14. P. G. Hill and C. R. Peterson, *Mechanics and Thermodynamics of Propulsion*, Addison-Wesley Publishing Company, Reading, MA, 1992.

- 19-15. E. L. Resler, Jr., and W. R. Sears, "Prospects of Magneto-Aerodynamics," *Journal of Aeronautical Sciences*, Vol. 24, No. 4, April 1958, pp. 235-246.
- 19-16. M. Martinez-Sanchez and J. E. Pollard, "Spacecraft Electric Propulsion—An Overview," *Journal of Propulsion and Power*, Vol. 14, No. 5, September–October 1998, pp. 688-699.
- 19–17. C. H. McLean, J. B. McVey, and D. T. Schappell, "Testing of a U.S.-built HET System for Orbit Transfer Applications," *AIAA Paper 99-2574*, June 1999.
- 19–18. V. Kim, "Main Physical Features and Processes Determining the Performance of Stationary Plasma Thrusters," *Journal of Propulsion and Power*, Vol. 14, No. 5, September–October 1998, pp. 736–743.
- 19-19. D. Baker, "Mission Design Case Study," in R. W. Humble, G. N. Henry, and W. J. Larson (Eds.), *Space Propulsion Analysis and Design*, McGraw-Hill, New York, 1995, Chapter 10.
- 19-20. J. J. DeBellis, "Optimization Procedure for Electric Propulsion Engines," MS thesis, Naval Postgraduate School, Monterey, CA, December 1999, 75 pages.
- 19-21. J. D. Filliben, "Electric Propulsion for Spacecraft Applications," *Chemical Propulsion Information Agency Report CPTR 96-64*, The Johns Hopkins University, December 1996.
- 19-22. M. A. Kurtz, H. L. Kurtz, and H. O. Schrade, "Optimization of Electric Propulsion Systems Considering Specific Power as a Function of Specific Impulse," *Journal of Propulsion and Power*, Vol. 4, No. 2, 1988, pp. 512-519.